First publ. in: International Review of Cytology 255 (2006), pp. 133-176

Sub-Second Cellular Dynamics: Time-Resolved Electron Microscopy and Functional Correlation

Helmut Plattner and Joachim Hentschel
Department of Biology, University of Konstanz,
78457 Konstanz, Germany

Subcellular processes, from molecular events to organellar responses and cell movement, cover a broad scale in time and space. Clearly the extremes, such as ion channel activation are accessible only by electrophysiology, whereas numerous routine methods exist for relatively slow processes. However, many other processes, from a millisecond time scale on, can be "caught" only by methods providing appropriate time resolution. Fast freezing (cryofixation) is the method of choice in that case. In combination with follow-up methodologies appropriate for electron microscopic (EM) analysis, with all its variations, such technologies can also provide high spatial resolution. Such analyses may include, for example, freeze-fracturing for analyzing restructuring of membrane components, scanning EM and other standard EM techniques, as well as analytical EM analyses. The latter encompass energy-dispersive x-ray microanalysis and electron spectroscopic imaging, all applicable, for instance, to the second messenger, calcium. Most importantly, when conducted in parallel, such analyses can provide a structural background to the functional analyses, such as cyclic nucleotide formation or protein de- or rephosphorylation during cell stimulation. In sum, we discuss many examples of how it is practically possible to achieve strict function-structure correlations in the sub-second time range. We complement this review by discussing alternative methods currently available to analyze fast cellular phenomena occurring in the sub-second time range.

KEYWORDS: Ca^{2+}, Calcium, Cryofixation, Electron microscopy, Endocytosis, Exocytosis, Membrane fusion.

I. Introduction

The cell as a dynamic, four-dimensional research object requires the availability of a spectrum of methodologies and tools to analyze properly structural and functional details over a broad range of temporal and spatial resolution. In fact, many attempts have been made in the literature to tackle the problem of analyzing dynamic processes in cells, from conformational changes of macromolecules to shape change of cells or of subcellular organelles—to mention just some extreme examples.

Very complex dynamic events, such as ciliary beat, exocytosis, and endocytosis take place on a sub-second time scale, including some very rapid steps, such as membrane fusion. They may be addressed by widely different methods, each of which will unravel specific details. For membrane fusion, one of the most demanding examples, extremely rapid recording by patch-clamp analysis is available (Dernick *et al.*, 2005; Neher and Marty, 1982), though any structural features of such events remain undetected. A most feasible way to achieve stringent structure-function correlation would be to exploit the high spatial resolution of the electron microscope (EM), including analytical methods (e.g., energy-dispersive x-ray microanalysis). The absence of any time resolution in the EM, however, requires physical fixation of precisely timed processes (Plattner and Bachmann, 1982; Sitte, 1996). The method of choice is fast freezing (cryofixation), which allows one to inactivate fast processes on a millisecond time scale, in combination with a variety of follow-up procedures for structural and functional analyses, including measurement of calcium dynamics and of biochemical parameters, such as cyclic nucleotide formation and protein (de-)phosphorylation. Examples of all these phenomena will be presented in this review.

Such combined techniques can be most favorably applied to cell cultures. Work in our laboratory has focused on cell suspensions, including synchronous exocytosis/endocytosis systems. However, from the literature we give examples for other work, such as with muscle cells during synchronous contraction induced by electrostimulation.

Many of the phenomena in focus are counter-regulated rapidly. This can hold for some de-/re-phosphorylation processes (Plattner and Kissmehl, 2005). Yet these steps can be dissected in cells synchronously triggered by mixing with a stimulant in a quenched-flow apparatus in combination with cryofixation. While biochemical analyses, such as second messenger formation, are easy to perform with rapidly frozen cells, this is much more difficult with some other phenomena, (e.g., calcium signaling) (Plattner and Klauke, 2001) for which we discuss useful preparation protocols in conjunction with subsequent analysis by EM-based x-ray microanalysis. The method described here is different from that successfully used with muscle cells in previous work (Somlyo *et al.*, 1981; Wendt-Gallitelli and Isenberg, 1991).

To combine the most important aspects, time resolution and synchronous stimulation, we have elaborated in our laboratory a quenched-flow technology that also allows one to process samples for EM analysis. The crucial aspect of the present review is to survey work connecting the gap between functional data and high resolution work based on EM analysis with all its repertoire of follow-up procedures.

II. Analytical Methods

A. Appreciation of Methods Available

Although a range of methods is available, possibilities to correlate structural and functional data have remained restricted. Commercial instruments are available for rapid flow technologies, including stopped-flow and quenched-flow (Dunford, 1983; Gore, 2000). Stopped-flow operates with short activation times, whereas quenched-flow allows stimulation of samples, also by rapid mixing with a stimulant, for different time intervals, followed by rapid quenching (Moffat and Henderson, 1995; Plattner and Bachmann, 1982). Stopped-flow techniques are used mainly to measure very rapid processes and, thus, require vigorous mixing with intense shearing forces. This technique serves preferably to determine enzyme kinetics (Cherepanov and DeVries, 2004; Gutfreund, 1999; Purich, 2002), protein folding (Kumar *et al.*, 2005), metabolite formation (Genazzani *et al.*, 1997), ligand-receptor interactions (Hess, 1993; Sklar *et al.*, 2002), second messenger generation (Knipper *et al.*, 1993) and Ca^{2+} signaling in cell fragments (Tareilus *et al.*, 1993) or isolated organelles (Lang and Bronk, 1978; Saiki and Ikemoto, 1999). In a combination of fast freezing and EM, conformational changes of macromolecules or aggregates thereof upon stimulation (Berriman and Unwin, 1994; Chestnut *et al.*, 1992; Moffat and Henderson, 1995; Unwin, 1995), notably of actomyosin (Hirose *et al.*, 1993; Pollard *et al.*, 1990, 1993; Walker *et al.*, 1999) could be studied. A computer-controlled spray-freezing apparatus with millisecond time-resolution, as designed by White *et al.* (1998), allows for the analysis of molecular interactions on EM grids.

Clearly many cells are mechanically sensitive and, therefore, may be severely affected by shearing forces occurring during vigorous mixing. Moreover, most complex cellular functions do not even require time resolution of the type provided by stopped-flow techniques. Altogether the type of cells and fast events, respectively, analyzed by quenched-flow methodology has remained restricted. One reason may be, in fact, impairment of cells by instruments commonly available. There are, however, some examples successfully analyzed with tailor-made variations of rapid-quenching methods.

Such work included electrically excitable cells, such as neuronal cell fragments (Pozzo-Miller *et al.*, 1999, 2000; Tareilus *et al.*, 1993) and intact neuronal cells (Heuser *et al.*, 1979; Torri-Tarelli *et al.*, 1985), as well as myocytes (Taylor *et al.*, 1999). Obviously excitable cells are generally more easily amenable to time-resolved analyses. Methods applied with these techniques included rapid optical [Ca^{2+}] recordings (Cheek *et al.*, 1994) and more frequently bulk freezing (cryofixation) in pace with stimulation, followed by structural and/or analytical evaluation at the EM level (Jorgensen *et al.*, 1988; Pezzati *et al.*, 2001; Pozzo-Miller *et al.*, 1999, 2000; Shattock *et al.*, 1998; Somlyo *et al.*, 1981; Wendt-Gallitelli and Isenberg, 1991).

Cryofixation in the present context means rapid freezing (Plattner and Bachmann, 1982; Sitte, 1996). This does not include high-pressure freezing, which requires at least fractions of a minute for sample taking, for example, from tissues (Vanhecke *et al.*, 2003), to freezing, without the possibility of timed stimulation. Furthermore, this technique essentially exploits the pressure-dependency of freezing according to the phase diagram of water (Moor, 1987), rather than quick freezing by high cooling rates.

Although important results have been achieved with cryofixation combined with electrical stimulation, this clearly remained of restricted applicability specifically to excitable cells. None of the methods available for timed sub-second cellular analyses has become established for broader use. There is a spectrum of more widely used methods which in part are rather indirect, and in part performed under microscope control. These include widely varying methods, from real-time Ca^{2-} imaging (Montell, 2005; Muallem, 2005; Rudolf *et al.*, 2004), pulse stimulation for caged compound-activation (Abelson *et al.*, 1998; Böhmer *et al.*, 2005; Politz, 1999; Wood *et al.*, 2005), to the most rapid electrophysiological techniques based on patch-clamp electrophysiology (Chow *et al.*, 1992; Henkel and Almers, 1996; Neher, 1998; Neher and Marty, 1982). These may eventually be combined with amperometric recordings of secretory contents release (Alés *et al.*, 1999; Burgoyne *et al.*, 2001; Dernick *et al.*, 2005), simultaneous measurement of presynaptic capacitance and postsynaptic currents (Sun and Wu, 2001), as well as some other techniques (Neher, 1998; Petersen *et al.*, 2005). For a more detailed account of recent developments, see Section IV.B.

For a broader applicability it was important to fill this gap, at least in part, with a methodology applicable to cell suspensions. Such work aimed at a combined structure/function analysis of membrane and organelle dynamics, (e.g., during stimulation and signal transduction). Quenched-flow technology offers itself for this purpose (Knoll *et al.*, 1991). This method largely depends (1) on adequate mixing of cells with a stimulant for variable times, and (2) on rapid inactivation which allows both adequate ultrastructural preservation and processing by (ultra-)structural and biochemical methods. The crucial element of such a device is a properly designed mixing chamber combined

with cryofixation, allowing for cooling rates as high as possible (Plattner and Bachmann, 1982). Beyond work with cells, as documented in this review mainly by work from our lab, this technical principle has recently been adapted to rapid kinetic analysis of proteins (Cherepanov and De Vries, 2004).

B. Principle of the Methodology Applicable to Cell Suspensions

A variety of follow-up procedures, notably EM analyses, can be combined with quenched-flow/cryofixation (Fig. 1). This in turn can be correlated with other methods, from electrophysiology, fluorescent dye analysis, Ca^{2+}, and second messenger analysis. Although EM techniques provide highest spatial resolution, they are not only time consuming, but they also lack any temporal resolution. This drawback can be overcome when dynamic processes, preferably in synchronous systems, are stopped at different time intervals after stimulation. For this, the method of choice is physical fixation, usually by rapid freezing (cryofixation) (Plattner and Bachmann, 1982; Sitte, 1996). EM analysis can include freeze-fracturing, freeze-substitution, transmission EM (TEM), and scanning EM (SEM), as well as analytical methods, such as electron spectroscopic imaging (ESI) (Bauer, 1988; Reimer, 1998) and energy-dispersive x-ray microanalysis (EDX) (Ingram *et al.*, 1999; Reimer, 1998), both allowing to localize elements, (e.g., total concentrations of calcium). All these follow-up procedures require different preparation protocols. Figure 1 summarizes the

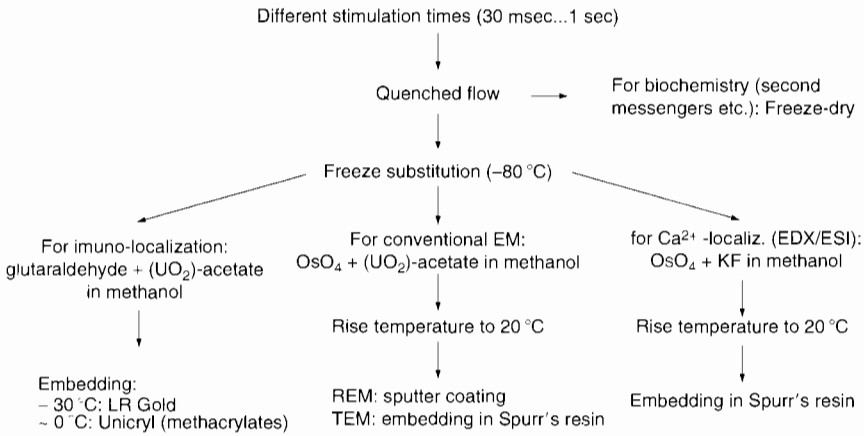

FIG. 1 Preparative pathways that can be applied after quenched-flow following different stimulation times. Widely different methods, such as (ultra-)structure analysis (eventually combined with analytical EM techniques, ESI, EDX) and biochemical measurements, can be combined.

technology used in our laboratory. In many cases, EM or light microscopical analyses can be complemented by measurement of calcium signals, of other second messengers, of phosphorylation states of proteins, etc.

The cryofixation method used (Fig. 2) is based on spray-freezing (Bachmann and Schmitt, 1971), which exploits the high surface-to-volume ratio when a cell is rapidly injected into a cryogen. This allows adequate preservation of cellular ultrastructure (Plattner *et al.*, 1972). In combination with a newly developed mixing chamber this allows for time-resolved analyses in the sub-second time range even with fragile cell suspensions (Knoll *et al.*, 1991) as follows. To achieve precisely timed samples, cell suspensions are rapidly mixed with a stimulant in a mixing chamber and sprayed into melting propane (−187°C) as a highly efficient cryogen. The tubing between the mixing chamber and the cryogen defines the trigger time (Knoll *et al.*, 1991). From a dead-time of 30 ms on, rather precisely timed samples can be prepared.

The potential use of a combined quenched-flow/cryofixation/follow-up technology can be exemplified briefly as follows. For example, it allows the assessment of the kinetics of exo-endocytosis coupling (Knoll *et al.*, 1991; Plattner *et al.*, 1992), as exemplified in Figs. 3–6. One can thus follow by freeze-fracturing the restructuring of membrane constituents during and after stimulated fusion (Knoll *et al.*, 1991). Aliquots of time series may be processed for an analysis of intracellular calcium distribution by ESI (Knoll *et al.*, 1993) and EDX (Hardt and Plattner, 1999; 2000; Husser *et al.*, 2004; Plattner *et al.*, 2006), as documented in Figs. 7–10. With a slightly extended equipment one can also rapidly manipulate the extracellular milieu, for instance, ionic conditions, and thus study its effect on exo-endocytosis performance (Plattner *et al.*, 1997), as shown in Fig. 11. Another example is second messenger formation during ciliary beat regulation (Yang *et al.*, 1997), as documented in Figs. 12 and 13. The analysis of rapid protein de-/re-phosphorylation is another application (Höhne-Zell *et al.*, 1992), of which Fig. 14 is an example.

To achieve such data by the methodology under consideration, synchronization of events is of paramount importance. It is equally important to note that cryofixation, as used in this context, cannot yield kinetic data on individual events. Even with timed sampling one looks only on a population of "reacting" organelles or of events. Also note that analytical EM methods, ESI and EDX, register local concentrations of total calcium, [Ca], which by far exceeds that of free, ionically dissolved Ca^{2+}, $[Ca^{2+}]$. Comparing both allows for important additional information.

C. A Useful Synchronous Biological System

To establish a quench-flow method applicable even to very sensitive cells, the ciliated protozoan, *Paramecium tetraurelia*, has been chosen. Therefore, this may now be the most thoroughly analyzed system. This selection is mainly

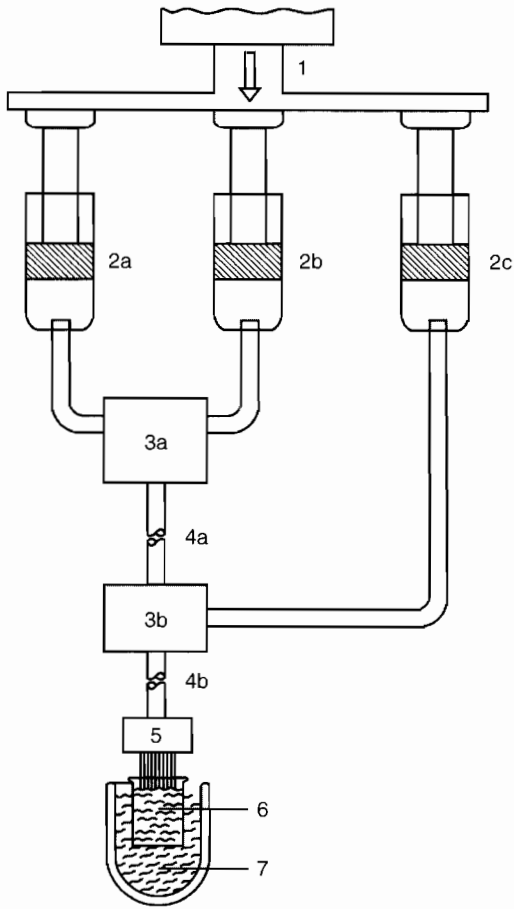

FIG. 2 Design of a quenched-flow apparatus with two mixing chambers. Modified after Knoll *et al.* (1991). *J. Cell Biol.* **113,** 1295–1304 by copyright permission of The Rockefeller University Press. A ram (1) is advanced under electronic control with a preselected pressure to push down the piston in the syringes (2). These contain different fluids, for example, from left to right: cells suspended in their culture medium, a Ca^{2+}-chelator (to adjust $[Ca^{2+}]_o$ to a preselected, controlled level), and a trigger solution. Mixing chamber 3a provides the respective $[Ca^{2+}]_o$ for a variable time (depending on the pressure applied and the geometry of tube 4a) before cells are stimulated in mixing chamber 3b. The actual trigger time depends again on pressure and geometry of the tube, 4b. A spray-nozzle (position 5, sieve plate with openings, e.g., of 30, 50, or 100 μm) allows the injection of cells as spray-droplets into melting propane (6) cooled with liquid N (7). While Ca^{2+} is chelated, Sr^{2+} can be substituted for Ca^{2+} in the mixing chamber 3a (Hardt and Plattner, 1999, 2000). In practice, the device will be used mainly with two mixing chambers only (cell suspension and activation solution).

due to its unsurpassed synchrony of dense-core vesicle exocytosis performance (Plattner and Kissmehl, 2003a; Plattner *et al.*, 1993) and the fact that its ciliary beat can also be easily manipulated—both being Ca^{2+}-dependent

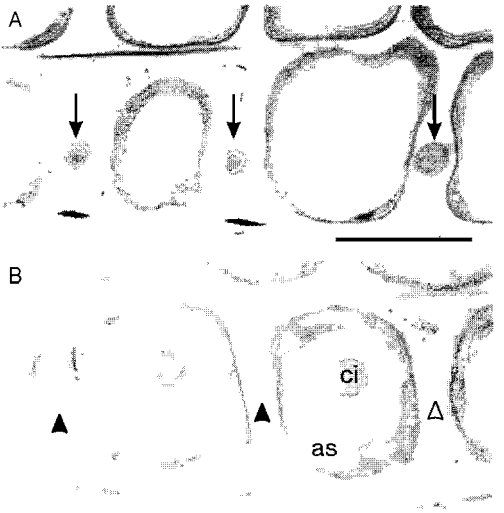

FIG. 3 Tangentional section through the surface of a *Paramecium* cell, (A) before and (B) 80 ms after stimulation of trichocyst exocytosis ($Ca^{2-}|_o$ = 1 mM). Quenched-flow, freeze-substitution, epoxide embedding, transmission-EM analysis. Note the regular arrangement of trichocysts before stimulation (arrows in A) and of ghosts (dark arrowheads) or empty docking sites in (clear arrowhead) after stimulation. To be compared with Fig. 5 Trichocysts or ghosts alternate with cilia (ci) emerging from depressions in the surface relief of the cell, and these depressions are outlined by cortical Ca-stores, the alveolar sacs (as). Bar = 1 μm. From Knoll *et al* (1991). *J. Cell Biol.* **113**, 1295–1304 by copyright permission of The Rockefeller University Press.

processes. These cells are ~100-μm long and ~40-μm thick. They are endowed with several thousand cilia and up to ~1000 dense-core secretory organelles (trichocysts) which they can release by exocytosis in response to the polyamine secretagogue, aminoethyldextran (AED) (Plattner *et al.*, 1984, 1985), synchronously within a sub-second time interval (Knoll *et al.*, 1991; Plattner *et al.*, 1997). Cilia and trichocysts occur in a highly regular arrangement at the cell surface. In a population of cells synchronously triggered under standard conditions and processed for quantification by EM analysis, as described later, all exocytotic events take place within ~80 ms, followed by endocytosis within a total 350 ms after stimulation (Knoll *et al.*, 1991), with apparent half-times of $t_{1/2}^{exo}$ = 57 ms and $t_{1/2}^{endo}$ = 126 ms, respectively (Plattner *et al.*, 1992) (see Fig. 6). Therefore, this is the fastest and most synchronous dense-core exocytosis system known (Plattner and Kissmehl, 2003a) when compared with other systems (Kasai, 1999).

In the context of this review it is worth anticipating that "alveolar sacs" are physiologically important cortical calcium stores (Länge *et al.*, 1995; Stelly *et al.*, 1991). They are closely apposed to the cell membrane that they line

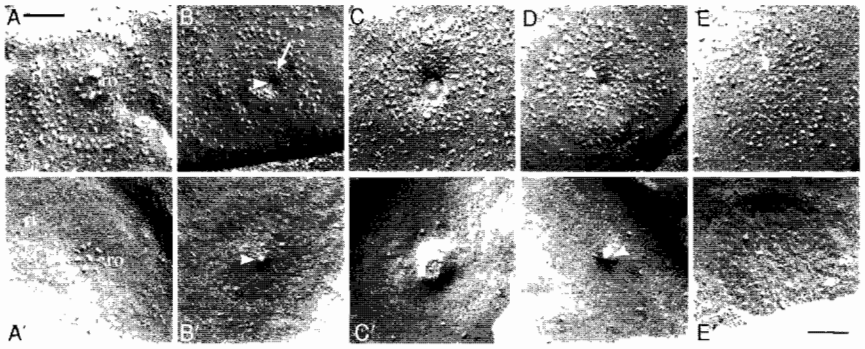

FIG. 4 Freeze-fracture analysis of changes occurring in the PF- (A–E) and the EF-face (A′ E′), respectively, of the *Paramecium* plasma membrane during stimulated trichocyst exocytosis. PF designates that part of the split cell membrane that remains with the cell body (A–E), while EF designates the centrifugal view on the half that is split away during fracturing (A′ E′). Note that these pictures from a series of quenched-flow experiments have been selected after establishing the time course for exo-/endocytosis coupling by ultrathin section analysis (see Figs. 5 and 6) and that the pictures shown are not complementary fractures from the same cell. Both views are combined because they may show different aspects in variable detail. (A, A′) are resting stages with a ring (ri), designating the exocytosis site, and a rosette (ro) of membrane particles (integral proteins) indicative of exocytosis competence in unstimulated cells. (B, B′) show formation of a focal fusion pore (arrowheads) and dispersal of small particles (arrow) which are thought to arise from the decay of rosette particles that disappear during exocytosis stimulation. (C, C′) contain a larger exocytotic opening, which can expand to the diameter of the ring. (D, D′) document that membrane resealing after exocytosis, that is during exocytosis-coupled endocytosis, is also of the focal type (arrowheads). (E, E′) represent the resealed state. Bar = 0.1 μm. Figures A–A′, B–B′, C–C′, and E–E′ from From Knoll *et al.* (1991). *J. Cell Biol.* **113**, 1295–1304 by copyright permission of The Rockefeller University Press. Figures D–D′ from Plattner *et al.* (1992). *J. Cell Sci.* **103**, 613–618 by copyright permission of The Company of Biologists.

over most of the cell surface area, with the exception of the sites where trichocysts are docked and where cilia emerge. Calcium dynamics in alveolar sacs is an important aspect also considered here (Figs. 7–10). The other aspect analyzed with *Paramecium* cells, ciliary beat, normally operates at ~20 Hz (Husser *et al.*, 2004). Depolarization of the surface membrane potential entails reversal of the ciliary beat (ciliary reversal), mediated by an influx of Ca^{2+} via the ciliary membrane (Machemer and Ogura, 1979). Depolarization and hyperpolarization can be chemically induced in the mixing chamber and samples analyzed for cyclic nucleotide formation (Yang *et al.*, 1997) or for ciliary calcium dynamics by EDX (Husser *et al.*, 2004; Plattner and Klauke, 2001; Plattner *et al.*, 2006), all within one ciliary stroke.

In *Paramecium*, the existence of numerous mutants, such as some without any Ca^{2-} influx upon exocytosis and/or ciliary reversal stimulation (Kerboeuf and Cohen, 1990) is of paramount importance. Just like *Paramecium*, any

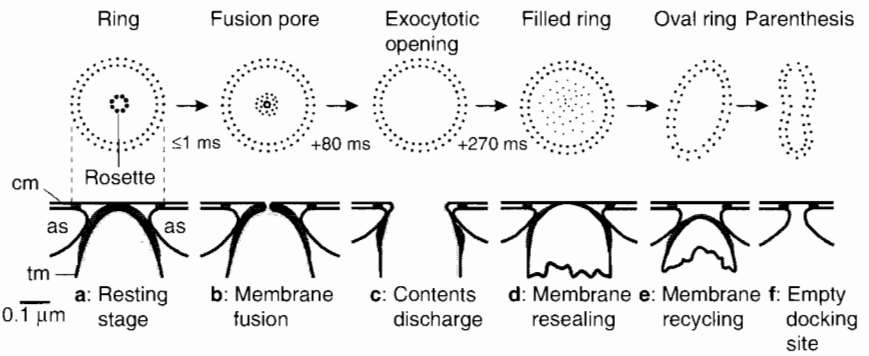

FIG. 5 Schematic presentation of the time course of trichocyst exocytosis and exocytosis-coupled endocytosis in *Paramecium*. For structures, like ring and rosette, as well as for their transformation during membrane fusion, see Fig. 4. After resealing, a filled ring is formed which then collapses to an oval ring and a parenthesis stage. as, Alveolar sacs (around a trichocyst docking site); cm, cell membrane. Times estimated for standard conditions ($[Ca^{2-}]_o$ = 1 mM) are from Knoll *et al.* (1991) and Plattner *et al.* (1992, 1993); yet consider that all steps shown are accelerated, within limits, by increasing $[Ca^{2+}]_o$. From Plattner *et al.* (1997). *J. Membr. Biol.* **158**, 197–208 by copyright permission of Springer Verlag.

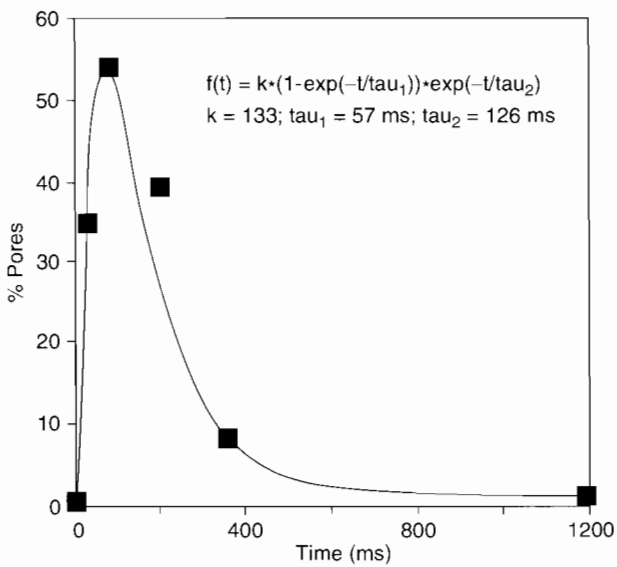

FIG. 6 Time course of trichocyst exo-endocytosis performance in *Paramecium* under standard conditions. Values indicated are for the entire number of cells and their docking sites analyzed, rather than for individual steps, as explained in the text. From Plattner *et al.* (1992). *J. Cell Sci.* **103**, 613–618 by copyright permission of The Company of Biologists.

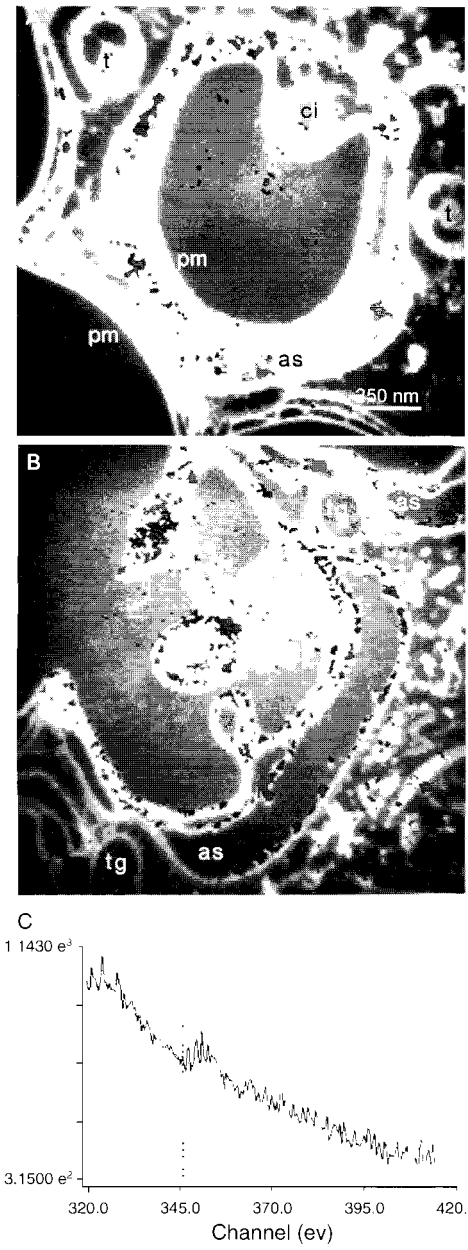

FIG. 7 ESI-based Ca-analysis in *Paramecium*. (A) before and (B) 80 ms after exocytosis stimulation. (C) is the energy loss spectrum with the Ca signal. For Ca imaging (displayed in red false color), as shown in (A) and (B), net signals after background subtraction have been used. Alveolar sacs (as) show Ca signals throughout their extension in (A), whereas after stimulation (B) Ca signals in alveolar sacs are restricted to their borders, with additional signals along the plasmamembrane (pm) and in cilia (ci). No Ca signals are seen in trichocysts (t) or trichocyst ghosts (tg). From Knoll *et al* (1993). *Cell Calcium*, **14**, 173–183 by copyright permission of Elsevier. (See also color insert.)

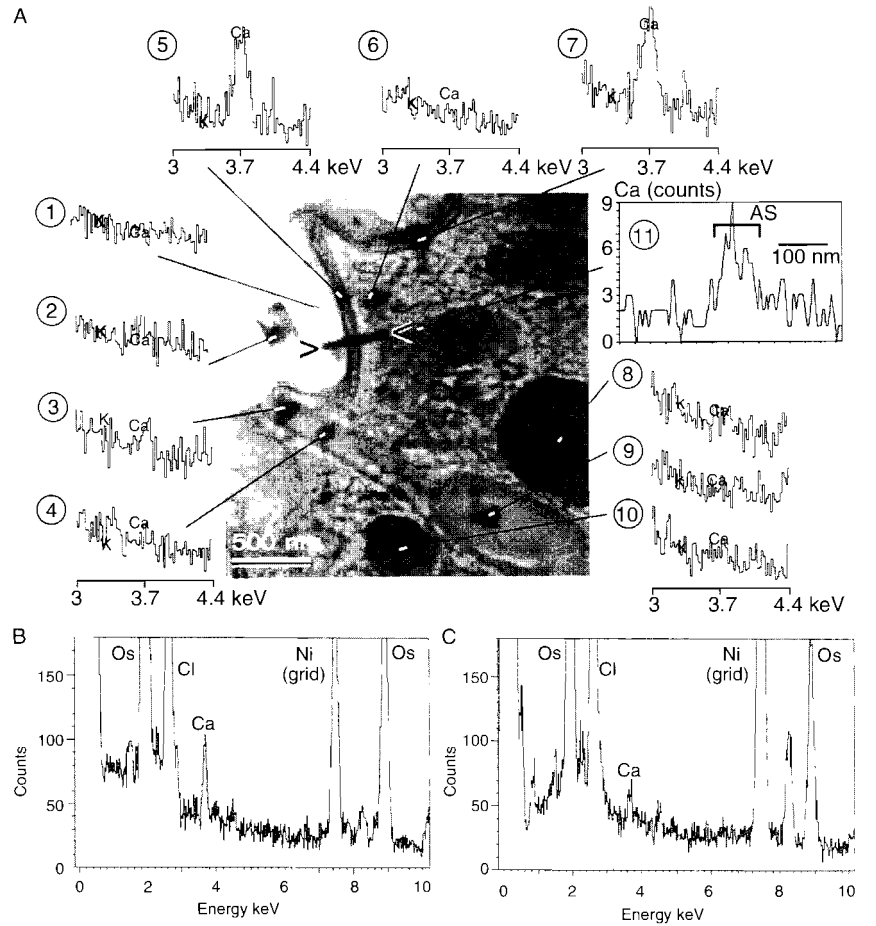

FIG. 8 Scanning transmission-EM (STEM) analysis of Ca^{2+} dynamics in *Paramecium*. (A) Cell cryofixed in the unstimulated state. STEM image from a 0.5-μm section, with dark dots and lines indicating positions of point measurements and line scan analysis. The outermost cell layer, delineated by electron-dense membrane systems in parallel arrangement at a distance of ~100 nm (top middle and top left), contains the alveolar sacs. The positions on alveolar sacs (5 and 7 in spot, 11 in line scan analysis) are the only ones yielding any significant CaKα signals, in contrast to measurements outside the cell (1), in a cilium (2), in upper (3, 4) or lower (9) trichocyst domains, cytosolic regions (6), and mitochondria (8, 10), respectively. The line scan (11) represents the distribution of CaKα signals along the analysis line (dark) with a peak over an alveolar sac. (B) Whole spectra (< 10 keV) recorded in alveolar sacs before and (C) 80 ms after trichocyst exocytosis stimulation. Note the change of the CaKα-signal in alveolar sacs after stimulation, disregarding peaks from preparative elements (Os, Cl, Ni). Quantitative evaluation of many calibrated spot measurements resulted in diagrams of the type shown in Figs. 9C and 10. (A) is from Plattner and Klauke (2001). *Intl. Rev. Cytol.* **201,** 115–208 by copyright permission of Elsevier; (B, C) are courtesy of M. Hardt and H. Plattner.

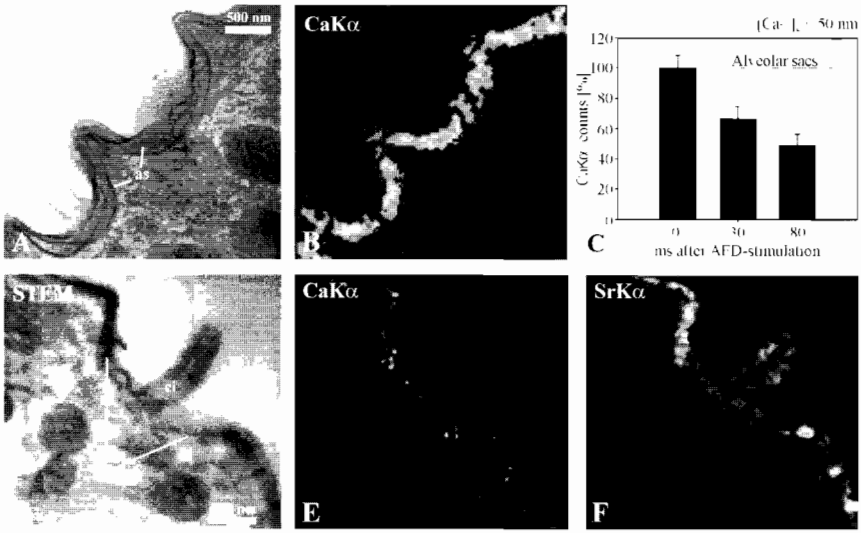

FIG. 9 EDX-based imaging of Ca and of Sr during exocytosis stimulation in *Paramecium*. (A) STEM image of unstimulated cell, with corresponding CaKα-distribution image (B), showing restriction of signals (in false colors, with some red hot spots) to alveolar sacs (as) and absence, for example from cilia (ci). (C) Decrease of net CaKα signals in alveolar sacs during exocytosis stimulation executed at $[Ca^{2-}]_0$ slightly below intracellular resting levels (see text). (D, E, F): STEM (D), CaKα (E) and SrKα image (F) of a cell AED-stimulated at low $[Ca^{2+}]_0$ in presence of an excess of Sr^{2+} added during stimulation. Note disappearance of the CaKα signal (E), whereas the SrKα signal emerges in alveolar sacs (and in the cilium). This clearly documents rapid release of Ca^{2+} from cortical stores and substitution of Sr^{2+} for Ca^{2+} in these stores, respectively, during exocytosis stimulation. (A–C) is from Hardt and Plattner. (2000) *Euro. J. Cell Biol.* **79**, 642–652 by copyright permission of Elsevier; (D–F) from Hardt and Plattner. (1999). *J Struct. Biol.* **128**, 187–199 by copyright permission of Elsevier. (See also color insert.)

other excitable cells in suspension can be analyzed by the quenched-flow method. In fact, the methodology under consideration could be of much broader use than noted in the literature. Peptidergic nerve terminals isolated from the posterior pituitary are an additional example (Knoll *et al.*, 1992b).

D. Preparative Aspects

In the quenched-flow device cells are rapidly mixed with the stimulant such that any mechanical disturbance is avoided (Knoll *et al.*, 1991) (Fig. 2). Precise timing of mixing and quenching has been ascertained by quantification of a color change reaction. Actual time resolution provided by spray-freezing, as mimicked with very small thermocouples, is estimated to be in the millisecond (ms) time range (Plattner and Bachmann, 1982). Before cells in suspension are

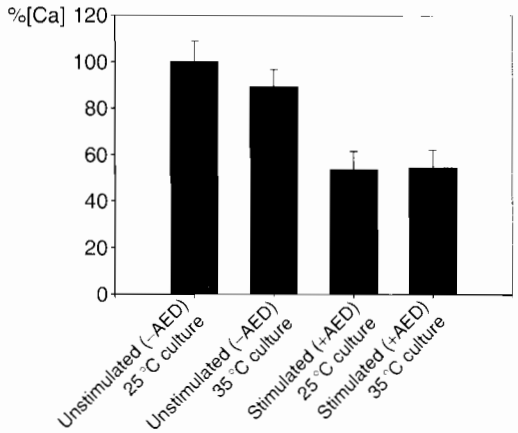

FIG. 10 EDX analysis of [Ca] in alveolar sacs of a temperature-sensitive *Paramecium* double mutant that allows for Ca^{2+} influx selectively via the nonciliary membrane when cultivated at 25 °C, but not after culture at 35 °C. Values are normalized to 100% for the nonstimulated 25 °C cells, but 35 °C cells display about the same [Ca] before stimulation. After stimulation [Ca] decreases by about the same percentage in both strains. This strictly argues against a Ca^{2+}-induced Ca^{2+}-release mechanism, as discussed in the text. Bars = s.e.m. Data derived from Mohamed *et al.* (2002).

stimulated, the extracellular calcium concentration, $[Ca^{2+}]_o$, may be briefly manipulated using ethyleneglycol tetraacetate (EGTA) as a rapid chelator (Bers *et al.*, 1994), $\tau \sim 0.2$ ms (see Plattner and Klauke, 2001, for a summary), as we eventually used it with *Paramecium* cells (Knoll *et al.*, 1993; Plattner *et al.*, 1997). Note that in biological systems normally the relation of $[Ca^{2+}]_o/[Ca^{2-}]_i$ is $\sim 10^4$ (Montell, 2005; Petersen *et al.*, 2005). For instance, with *Paramecium* cultures $[Ca^{2+}]$ in the medium is normally adjusted to between 50 and 500 μM, but may be lowered in the quenched-flow device within a millisecond to 30 nm, that is, about half of the level of free calcium within resting cells ($[Ca^{2-}]_i^{rest}$), as determined by fluorochrome analysis (Klauke and Plattner, 1997). This allows one to analyze selectively the contribution of the internally mobilized calcium pool to Ca^{2+} signaling. In a complementary approach Sr^{2-} has been substituted for $Ca^{2+}{}_o$, using the same buffers with known kinetics (Hardt and Plattner, 1999, 2000). This in turn allows one to assess, for instance, store refilling superimposed to mobilization during stimulation. In fact, this seems to be a unique opportunity to cope with the problem of superimposed rapid store mobilization and refilling (see Section III.D). All these manipulations, including subsequent stimulation, may be consecutively executed within 1 s or fractions thereof (Fig. 2).

Follow-up procedures that can be combined with this quenched-flow/cryofixation methodology (Fig. 1) include (1) freeze-fracture replication,

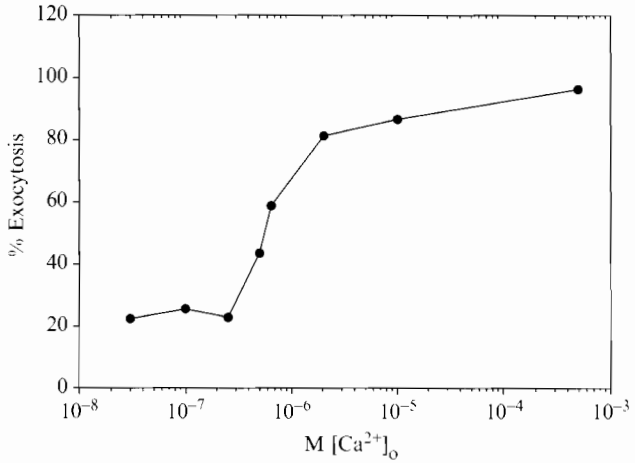

FIG. 11 Quenched-flow/freeze-fracture analysis of the dependency of trichocyst exocytosis in *Paramecium* on $[Ca^{2+}]_o$ adjusted by chelators as described by Mohamed *et al.* (2003). *Cell Calcium* **34,** 87–96 by copyright permission of Elsevier.

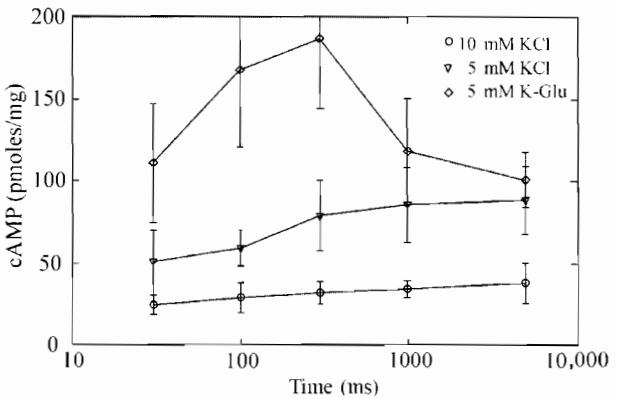

FIG. 12 Quenched-flow analysis in *Paramecium* of cAMP formation during strong (10 mM KCl) and weak (5 mM KCl) depolarization, respectively, and absence of cAMP formation during exposure to a KCl-glutamate solution (5 mM K-Glu) for the short period of time analyzed. Note that a ciliary stroke would require ~50 ms (see text) and that with 10 mM KCl cAMP rises already within one ciliary stroke (logarithmic time scale). Bars = s.e.m. From Yang *et al.* (1997). *J. Cell Sci.* **110,** 2567–2572 by copyright permission of The Company of Biologists.

(2) freeze-substitution for morphological REM or TEM analysis, (3) freeze-substitution for element analysis, (e.g. under conditions whereby Ca^{2+} is retained in place [see following]), (4) different types of functional analyses,

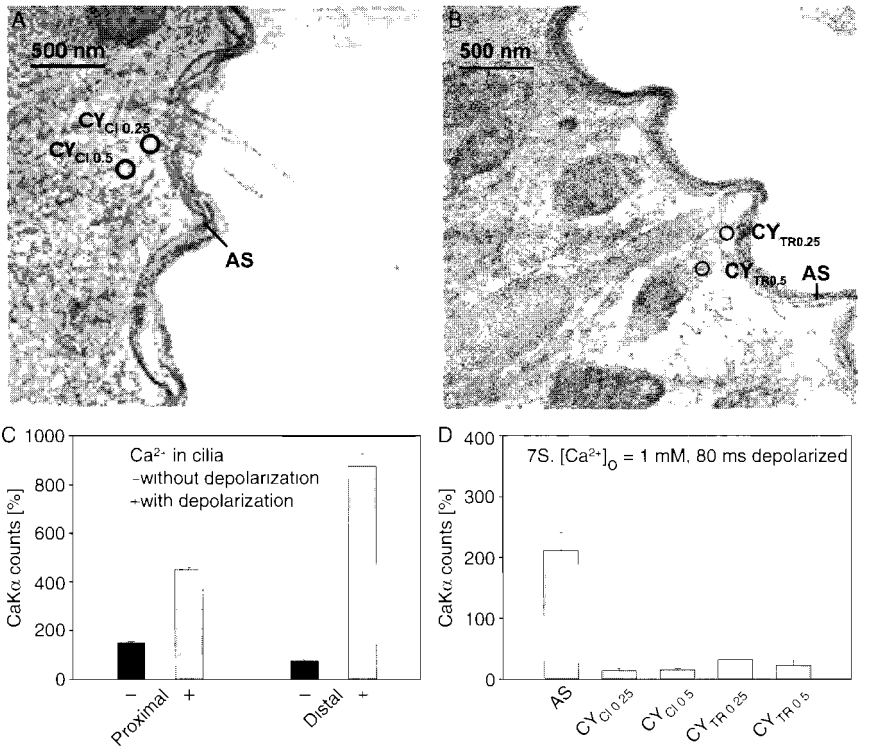

FIG. 13 EDX analysis of [Ca] increase in cilia of *Paramecium* after 80-ms depolarization (20-mM KCl, $[Ca^{2-}]_0$ = 1 mM) and absence of spill-over into nearby cytosol. (A, B) STEM images, (C, D) CaKα counts. Symbols $CY_{CI0.25}$, $CY_{CI0.5}$, $CY_{TR0.25}$, and $CY_{TR0.5}$ indicate cytosolic values determined near ciliary bases (CI) and trichocyst docking sites (TR) at a distance of 0.25 and 0.5 μm, respectively. For controls, aliquots were passed through the quenched-flow apparatus without KCl added. Note specific increase of [Ca] in cilia after depolarization, with some enrichment in a more distal region. Bars = s.e.m. Data compiled from Husser *et al* (2004) and unpublished results.

etc. These may include the determination of rapidly changing phosphorylation states by gel electrophoresis combined with autoradiography (Höhne-Zell *et al.*, 1992), of the formation of second messengers (Yang *et al.*, 1997) or of [Ca] dynamics by analytical EM techniques (ESI, EDX).

With respect to ESI and EDX analysis of [Ca] dynamics (Figs. 7–10, 13), retention of [Ca] in the untriggered state or in its distributed form after different trigger times is mandatory. This is possible by using a freeze-substitution medium containing fluoride (Hardt and Plattner, 1999, 2000; Knoll *et al.*, 1993) because CaF_2 has very low solubility. The same holds for Sr^{2+}, although SrF_2 is somewhat more soluble than CaF_2. After resin

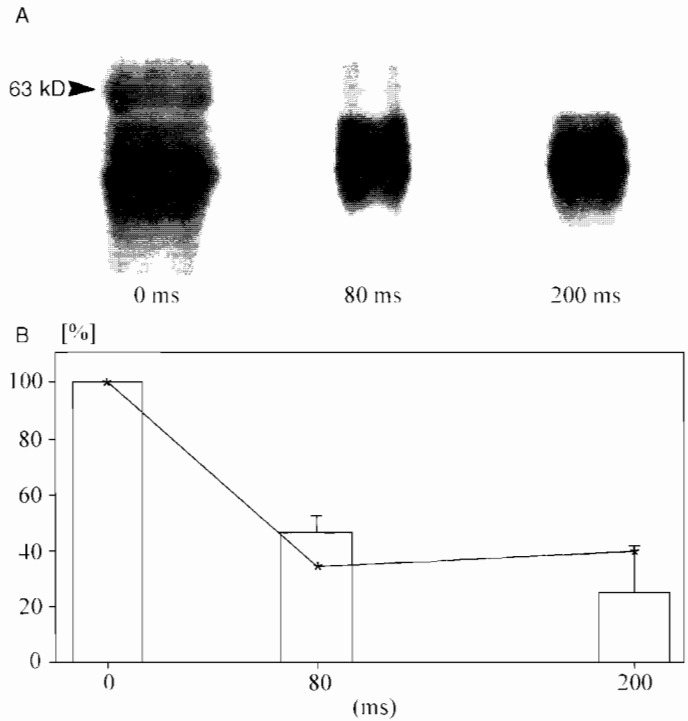

FIG. 14 Assessment of rapid (80 ms) dephosphorylation of a 63 kD-protein (pp63/pf) in *Paramecium* by quenched-flow during synchronous exocytosis induction. (A) Autoradiogram obtained after metabolic ^{32}P-labeling followed by SDS-polyacrylamide gel-electrophoresis. (B) Blocks, averaged pp63/pf dephosphorylation; line, extent of exocytosis observed in the same experiments; bars = s.e.m. From Höhne-Zell *et al.* (1992). *Biochem. J.* **286,** 843–849 by copyright permission of The Biochemical Society.

embedding and polymerization, samples can be analyzed by ESI (Knoll *et al.*, 1993), or by EDX (Hardt and Plattner, 1999, 2000; Husser *et al.*, 2004; Mohamed *et al.*, 2002, 2003; Plattner *et al.*, 2006). [Ca] values thus recorded exceed values of $[Ca^{2+}]_i$ in unstimulated cells by $\sim 10^4\times$ in *Paramecium* (Plattner and Klauke, 2001), just like in mammalian cells (Takahashi *et al.*, 1999). With *Paramecium* cells the applicability of calcium precipitation by fluoride ions, F^- (atomic weight = 19), during freeze-substitution, has been shown to be possible without redistribution artifacts (Hardt and Plattner, 1999). Previous work with *Paramecium* (Schmitz and Zierold, 1989) and several other cells (for examples see Section II.A) have used freeze-dried sections and, thus, relied on sublimation of H_2O (MW = 18). The considerably improved recognition of structural detail in freeze-substituted and plastic-embedded samples is a crucial advantage for precisely localized [Ca]

TABLE I
Characteristics of Processes Analyzed with Cells in Suspension

Process	Cell type	Time/Method	References
Ciliary beat			
Time for one beat	*Paramecium*	40 ms, video	(Husser *et al.*, 2004)
Exo-endocytosis			
Entire process	*Paramecium*	350 ms, quenched-flow/EM	(Knoll *et al.*, 1991)
Exocytosis	*Paramecium*	80 ms, quenched-flow/EM	(Knoll *et al.*, 1991)
Endocytosis	*Paramecium*	270 ms, quenched-flow/EM	(Knoll *et al.*, 1991)
Exo-endocytosis	Peptidergic nerve terminals	~300 ms, quenched-flow/EM	(Knoll *et al.*, 1992b)

EM, Electron microscopy.

determinations in small structural elements. The preparation protocol used is that presented in Fig. 1. Examples of the respective problems, methods, and solutions achieved are summarized in Tables I and II.

Quenched-flow may not necessarily be combined with cryofixation. An example is experiments on exo-endocytosis coupling with peptidergic nerve endings, which can be isolated from the rat posterior pituitary gland as viable cell fragments and activated by chemical depolarization in the quenched-flow device (Knoll *et al.*, 1992b). In that case, horseradish peroxidase (POX) has been added as a fluid-phase endocytosis marker to the medium before stimulation by exposure to high $[K^+]_o$ in the quenched-flow device. Inactivation by spraying into 0°C medium was followed by routine EM demonstration of the POX reaction product and counting of POX-positive vesicles at different time intervals after stimulation.

Paramecium cells have been subjected not only to AED-stimulation, but also to chemical depolarization or hyperpolarization, to analyze formation of cyclic guanosine monophosphate (cGMP) and cyclic adenosine-monophosphate (cAMP), respectively (Yang *et al.*, 1997). Samples were freeze-dried for further evaluation. Depolarization-induced ciliary reversal has been followed up also by EDX analysis of local [Ca] changes, notably in cilia (Husser *et al.*, 2004; Plattner *et al.*, 2006). In all these cases, cryofixation has been applied. The quenched-flow methodology has also been used for $^{45}Ca^{2-}$ flux measurements with high time-resolution with *Paramecium* cells which, in this case, have been sprayed into a 0°C medium for liquid scintillation counting (Knoll *et al.*, 1992a). As outlined in Section IV.B, there are some other examples of the application of quenched-flow technology to cell suspensions, yet without combination with EM analysis. In summary, quenched-flow experiments are not necessarily always to be combined with fast freezing.

TABLE II

Problems Analyzed with Cells in Suspension Using Quenched-Flow/EM and Correlated Functional Analysis

Process	Organism	Problem	Follow-up techniques	Reference
Exocytosis	*Paramecium*	Membrane fusion (pore formation)kinetics	Freeze-fracture	(Knoll *et al.*, 1991)
Exocytosis-coupled endocytosis	*Paramecium*	Membrane resealing	Freeze-fracture	(Knoll *et al.*, 1991; Plattner *et al.*, 1992)
		Protein (de-)phosphorylation	Biochemistry	(Höhne-Zell *et al.*, 1992)
		Ca^{2} as driving factor	Freeze-fracture	(Plattner *et al.*, 1997)
	Peptidergic nerve terminals	Kinetics	Peroxidase uptake	(Knoll*et al.*,1992b)
Ca^{2} dynamics during exocytosis	*Paramecium*	$^{45}Ca^{2}$ influx	Flux measurements	(Kerboeuf and Cohen, 1990; Knoll *et al.*, 1992a)
		Ca-store mobilization	ESI/EDX	(Hardt and Plattner, 2000; Mohamed *et al.*, 2002)
Ciliary beat	*Paramecium*	cAMP and GMP formation	Biochemistry	(Yang *et al.*, 1997)
		Ca^{2+} dynamics	EDX	(Husser *et al.*, 2004)

E. Analytical EM Methods

We have performed ESI and EDX analyses, respectively, with a Zeiss EM902 and Zeiss EM912 Omega instrument, respectively. Conditions used for ESI were as specified by Knoll *et al.* (1993), those for EDX with a Li-drifted Si detector were as specified by Hardt and Plattner (1999, 2000). Briefly, for ESI, ultrathin sections of dark gray interference color, only ~30- to 40-nm thick to avoid multiple excitation, were picked up on a 50-mM KF solution on uncoated grids. For any further details, see Knoll *et al.* (1993) and later. For EDX semithin sections of ~500-nm thickness were analyzed in the scanning transmission-EM (STEM) mode (80 kV, 10-μA beam current, 63-nm primary spot size, with a calculated top → bottom spread to 74 nm). This is appropriate for analyses of [Ca] in the cortical calcium stores, the alveolar sacs, and for changes in cilia whose dimensions relative to EDX resolution are sufficiently small (Table III). To discriminate between the different Me^{2+} pools during activation, one can perform rapid Ca^{2+}/Sr^{2+} replacement experiments in the quenched-flow apparatus (Hardt and Plattner, 1999, 2000). Substituting Sr^{2+} for Ca^{2+} is feasible, considering the body of literature showing similarity of effects (Hardt and Plattner, 2000), including store mobilization (Zoghbi *et al.*, 2004). These experiments can profit from the favorable energy resolution, with CaKα = 3.691 keV and SrKα = 14.143 keV. Quantitation of [Ca] in millimoles per Liter (mM/L) was achieved by

TABLE III
Key Values of *Paramecium* Cells Pertinent to Exocytosis Regulation

Average cell volume	7.33×10^4 μm^3	(Erxleben *et al.*, 1997)
Average width/volume of alveolar sacs	98 nm/~10^3 μm^3	(Erxleben *et al.*, 1997; Hardt and Plattner, 1999, 2000)
[Ca] in alveolar sacs	43 mM	(Hardt and Plattner, 1999, 2000)
Detection limit for [Ca] in *Paramecium* by EDX	2 mM	(Hardt and Plattner, 1999)
Time required for synchronous exocytosis	80 ms	(Knoll *et al.*, 1991)
Proportion of Ca released from cortical stores, 80 ms		
(exocytosis stimulation at $[Ca^{2+}]_o = 30$ nM)	40%	(Hardt and Plattner, 2000)
Proportion of Ca released from cortical stores during 1 s stimulation at $[Ca^{2+}]_o = 500$ μM		
Wild-type cells	~80%	(Hardt and Plattner, 2000)
Mutant without stimulated Ca^{2-} influx	~45%	(Mohamed *et al.*, 2002)
Relative contribution of Ca^{2+} mobilized from stores	~50%	(Plattner and Klauke, 2001)
Relative contribution of Ca^{2-} from influx	~50%	(Plattner and Klauke, 2001)

EDX evaluation of DeBruijn- and Chandler-type standards (as cited by Hardt and Plattner, 1999), that is, ion exchanger beads and epoxide matrix embedding, respectively. For additional controls, samples were evaluated also by neutron activation and atomic absorption (Hardt and Plattner, 1999).

III. Problems Solved by Correlated Time-Resolved EM and Functional Analyses

One can address specifically the following problems (Tables I, II). How and on which time scale are membranes restructured during fusion and fission, (e.g., during exo- and endocytosis, respectively)? This has been discussed in view of ongoing controversies on fusion pore formation (Jahn *et al.*, 2003; Martin, 2003; Mayer, 2002; Söllner, 2003). How is the cross-connection between internal and external Ca^{2+} sources during exo- and endocytosis? The dynamic coupling of (cortical) calcium stores to the cell membrane is particularly intensely debated up to the present time (Ambudkar, 2006; Berridge *et al.*, 2000, 2003; Rizzuto and Pozzan, 2006; Rosado *et al.*, 2005). Signaling within cilia during beat regulation has been analyzed, starting from within one beat cycle. In the latter case it was an open question how fast the respective cyclic nucleotides are formed during depolarization and hyperpolarization (Yang *et al.*, 1997), respectively, and how [Ca] is down-regulated altogether after ciliary reversal induction (Husser *et al.*, 2004; Plattner *et al.*, 2006).

A. Membrane Fusion and Fission

To have a chance to see any rapid process, some degree of synchrony is highly favorable. For instance, exocytosis can be reasonably analyzed by freeze-fracture EM in a quantitative way only if it can be stimulated in a highly synchronous manner. In *Paramecium*, dense core vesicles, known as trichocysts, are regularly arranged at the cell surface (Fig. 3). Exocytosis in response to AED occurs within 80 ms (Knoll *et al.*, 1991), but this characterizes all events in a synchronously reacting cell population, rather indicating the time required for the individual event which is much shorter.

A positive aspect specifically of quenched-flow/EM analysis is the possibility to see ultrastructural changes on freeze-fractures passing through membranes during fusion and resealing (Figs. 4, 5). This includes the following observation. Integral membrane proteins ("rosettes") positioned in the plasmamembrane at membrane fusion sites undergo dispersal into subunits during exocytosis (Knoll *et al.*, 1991). Rosettes are prerequisite to exocytotic membrane fusion and they assemble in dependency of the SNARE-specific

chaperone NSF (Froissard *et al.*, 2002; Kissmehl *et al.*, 2002). The time course of exo-endocytosis coupling, derived from quenched-flow experiments and quantitative freeze-fracture EM analysis, can be seen in Fig. 6.

Considering current uncertainty on pore-forming molecules, what may be the implications of these results? Formation of a narrow fusion pore, which then expands, has been first described by Heuser *et al.* (1979), based on correlated neuronal stimulation, fast-freezing and freeze-fracture analysis. Active participation of integral and peripheral proteins had been derived from work with *Paramecium* in an extended model called "focal fusion" (or point fusion), (Plattner, 1981). This has been based on the fact that mutants without the characteristic ultrastructural features at preformed exocytosis sites are unable to secrete their organelles although they contain them in great numbers docked at the cell membrane. Later on, a membrane fusion model operating by dispersing subunits of so far unidentified protein(s) has been propagated based on electrophysiological recordings (Almers, 1990). Quenched-flow/freeze-fracture analyses have shown the decay of rosette particles during focal fusion into six subunits (Knoll *et al.*, 1991). This appeared compatible with the fusion model derived from electrophysiology.

More specifically, SNAREs (SNAP receptors, SNAP = soluble NSF attachment proteins, NSF = N-ethyl maleimide–sensitive factor) (Jahn and Südhof, 1999; Rothman and Söllner, 1997) and more recently V_0 basepieces of fragmentary H^+-ATPase molecules lacking a catalytic part (Mayer, 2002; Peters *et al.*, 2001) have been discussed up to now as fusion pore-forming proteins. Although the assembly of rosette particles during trichocyst docking requires the SNARE-specific chaperone, NSF (Froissard *et al.*, 2002) and different SNAREs are identified as the *Paramecium* genome project proceeds (Plattner and Kissmehl, 2003b), this does not necessarily legitimize them to act as pore-forming agents during membrane fusion. Are time-resolved freeze-fracture data appropriate to support one or the other hypothesis on membrane fusion?

In general, SNARE proteins are located, in part, on the secretory vesicle membrane (v-SNAREs, e.g., synaptobrevin) and, in part, on the cell membrane acting as the target membrane (t-SNAREs, e.g., syntaxin and SNAP-25). A pin-like arrangement of several v-SNAREs and t-SNAREs mediates interaction of adjacent membranes. Only synaptobrevin and syntaxin are anchored in the respective membrane by a carboxy-terminal trans-membrane domain (Salaün *et al.*, 2004) and, thus, would be amenable to visualization by freeze-fracture EM. Generally, at this time, SNARE pins are considered the favorite candidates not only for membrane-to-membrane docking, but also for executing membrane fusion (Jahn *et al.*, 2003; Martin, 2003; Söllner, 2003).

In *Paramecium*, the existence of synaptobrevin (Schilde *et al.*, 2006) and of syntaxin homologues has been documented. An isoform of the latter occurs specifically in the cell membrane (Kissmehl *et al.*, submitted). Considering

the diameter of one transmembrane stretch (Eskandari *et al.*, 1998; Plattner and Zingsheim, 1983) one can estimate the number of molecules required to make up a freeze-fracture particle, such as a rosette particle at a trichocyst docking/fusion site (Plattner and Kissmehl, 2003a). The number thus calculated does not fit the assumptions made by others for the number of syntaxin molecules per fusion event. However, the estimations available for the stoichiometry of SNARE proteins do not appear sufficiently reliable for such correlations. Moreover, new arguments arise, including the hypothesis that syntaxin alone would line fusion pores (Han *et al.*, 2004). If so, this could theoretically also explain why no counterparts of rosette particles are seen on the secretory vesicle (trichocyst) membrane.

At this time, SNAREs can be reasonably assumed to participate in the formation of trichocyst exocytosis sites (see earlier). Recent analyses aimed at identifying and localizing the other proteins currently discussed as potential candidates for fusion pore formation, that is V_0 subunits of the H^+-ATPase (Mayer, 2002; Peters *et al.*, 2001), in *Paramecium* (Wassmer *et al.*, 2005). This hypothesis has received some support, but it has also been questioned. Support comes from work with synaptic vesicle release in *Drosophila* (Hiesinger *et al.*, 2005). In contrast, by expressing the different endogenous isoforms of relevant subunits as fluorescent fusion proteins in *Paramecium* we could largely exclude their occurrence at trichocyst exocytosis sites (Wassmer *et al.*, 2005) where they should have shown up in the characteristic regular spacing. Therefore, the identity of intrinsic membrane proteins undergoing restructuring in activated exocytosis sites (Fig. 4) still requires more scrutinized analysis, in *Paramecium* just as in other cells.

Another advantage of the application of the methodology described is the accessibility of fast exo-endocytosis coupling to both structural analysis and Ca^{2+} signaling (Plattner *et al.*, 1992, 1997). This was rewarding because for technical reasons endocytosis could not be captured by patch-clamp analysis for a long period of time (Rosenboom and Lindau, 1994). In particular, large cells have not been accessible to patch-clamp analysis for a considerable time. (With *Paramecium* it is still the case, not to speak of the pronounced surface profile and high rigidity of a *Paramecium* cell.) Just like in exocytosis, membrane fusion (resealing) during endocytosis in *Paramecium* is of the focal fusion type (Plattner *et al.*, 1992) (see Fig. 4). The focal kind of endocytotic membrane resealing is now assumed for any other system, based on patch-clamp analyses (Rosenboom and Lindau, 1994). Structurally this process is by no means a reversal of exocytotic fusion because rosette subunits remain dispersed (Knoll *et al.*, 1991; Plattner *et al.*, 1992, 1997). The performance and molecular machinery involved are also essentially different from those governing exocytosis (Conner and Schmid, 2003), though endocytosis also involves SNARE proteins (Gurunathan *et al.*, 2002; Séron *et al.*, 1998). Endocytosis generally follows exocytosis within a second or so in

Paramecium (Fig. 6), just like in other cells (Krupa and Liu, 2004). Again precise timing of the analyses is important.

Based on the methodology described, the overall time course of exo-endocytosis coupling in *Paramecium* (Knoll *et al.*, 1991; Plattner *et al.*, 1992) and in peptidergic pituitary cell fragments (Knoll *et al.*, 1992b) varies between 0.35 and several seconds, respectively. This is within the frame found by other methods in systems practicing the "kiss-and-run" type of exo-endocytosis coupling (Gandhi and Stevens, 2003; Henkel *et al.*, 2001; Palfrey and Artalejo, 1998; Taraska *et al.*, 2003; Wu, 2004), whereas previous estimates were by orders of magnitude too long. Comparison of different methods is also useful particularly given that conditions may vary depending on the system analyzed (Krupa and Liu, 2004). In *Paramecium*, the entire exo-endocytosis cycle is accomplished in the sub-second time range (Figs. 5, 6), with complete release of the rather bulky secretory contents.

B. Calcium Dynamics During Exo- and Endocytosis

Using quenched-flow/freeze-fracture analysis, the time course of exocytosis and of ensuing endocytosis (synchronized individual events in a population of cells) has been analyzed in *Paramecium* in dependency of $[Ca^{2-}]_o$ (Plattner *et al.*, 1997). All steps of the trichocyst release cycle (Fig. 5), from exocytotic membrane fusion (Fig. 11) to endocytotic resealing are accelerated (within limits) by increasing $[Ca^{2-}]_o$. This resembles findings with a variety of other cell types by alternative methods (Alés *et al.*, 1999; Kavalali *et al.*, 1999; Rosenboom and Lindau, 1994; Teng and Wilkinson, 2003; Thomas *et al.*, 1990; Wang *et al.*, 2006). Beyond that, with the application of quenched-flow to *Paramecium* cells, the removal of empty ghost membranes from the cell periphery could be analyzed. Also this step is found to be accelerated by increasing $[Ca^{2+}]_o$ (Plattner *et al.*, 1997). In other cells, this step which is much slower than the preceding ones, could be analyzed only more recently by using fluorescent labeling and total internal reflection microscopy (Yarar *et al.*, 2005) (see Section IV.B).

A most important aspect in cell biology is the microdomain dynamics of Ca^{2+} signals operating as a second messenger in widely different processes (Ambudkar, 2006; Barclay *et al.*, 2005; Berridge, 1998; Berridge *et al.*, 2000, 2003; Rizzuto and Pozzan, 2006; Rosado *et al.*, 2005). This includes specifically exocytosis (Neher, 1998), exocytosis-coupled endocytosis (Alés *et al.*, 1999; Kavalali *et al.*, 1999; Rosenboom and Lindau, 1994; Teng and Wilkinson, 2003; Thomas *et al.*, 1990), and ciliary beat activity (Machemer, 1988; Preston and Saimi, 1990).

When *Paramecium* cells are stimulated for exocytosis in presence of $^{45}Ca^{2+}$, this can be combined with $^{45}Ca^{2+}$ flux measurements (Knoll *et al.*, 1992a)

by the use of quenched-flow (rapid cooling without freezing). The "cryo-" variation of this methodology can be combined with ESI (Knoll *et al.*, 1993; Fig. 7) and EDX analyses (Hardt and Plattner, 1999, 2000; Plattner and Hardt, 2000; Figs. 8–10). During exocytosis Ca^{2+} is mobilized from cortical stores as the primary event (Fig. 9C), paralleled by store-operated Ca^{2+}-influx (SOC) as a second step (Hardt and Plattner, 2000), in line with fluorochrome analysis (Klauke *et al.*, 2000). This aspect will be discussed in more detail in Section III.D.

C. Signaling During Ciliary Beat Regulation

Second messenger generation has also been analyzed during ciliary beat regulation in *Paramecium*. Ciliary beat operates at ~20 Hz. Chemical hyper- and depolarization in quenched-flow experiments, from 30 ms on, were combined with cAMP and cGMP determinations (Yang *et al.*, 1997; Fig. 12). Hyperpolarization, which speeds up ciliary beat frequency and, thus, forward movement, causes an increase of cAMP (Pech, 1995; Preston and Saimi, 1990). In contrast, depolarization causes an influx of Ca^{2+} from the outside medium into cilia (Machemer and Ogura, 1979; Preston and Saimi, 1990; Tamm, 1994; Tamm and Terasaki, 1994), which entails a rise in cGMP (Majima *et al.*, 1986) due to Ca^{2+}-dependent guanylate cyclase activation (Schultz and Klumpp, 1993). The same occurs during AED stimulation, from ~0.5 s on (Knoll *et al.*, 1992a), remarkably due to a spill-over of Ca^{2+} from nonciliary domains into cilia (Husser *et al.*, 2004). Most likely the concerted effects of Ca^{2+}, cAMP, or cGMP (Majima *et al.*, 1986; Nakaoka and Machemer, 1990; Pech, 1995) can activate in cilia protein kinases with the respective sensitivities and thus regulate ciliary activity (Hamasaki *et al.*, 1991; Kim *et al.*, 2002; Preston and Saimi, 1990; Schultz and Klumpp, 1993). According to quenched-flow analysis, depolarization causes cAMP formation (Yang *et al.*, 1997) and $[Ca^{2+}]_i$ increase (Husser *et al.*, 2004), both within one beat cycle, while cGMP is formed during depolarization with some delay (Yang *et al.*, 1997).

Concerning calcium dynamics during ciliary activity regulation, the following results have been obtained by timed chemical depolarization (high K^+-media) in conjunction with quenched-flow/EDX analyses (Fig. 13). Depending on conditions of extracellular Ca^{2+}, depolarization can cause a rapid increase of [Ca] along the entire cilium (Husser *et al.*, 2004; Plattner *et al.*, 2006). This may preclude selective enrichment of voltage-dependent Ca^{2+} channels in certain domains of a cilium. (So far, these channels are characterized only by electrophysiology and not yet amenable to immunolocalization.) Under over-stimulation conditions (see Section III.D) [Ca] values registered by EDX in cilia after depolarization can become about as high as in alveolar sacs or even higher. Such values are compatible with the Ca^{2+}-fluxes

registered by electrophysiology if one takes into account the Ca^{2+}-flux into adjacent cell cortex domains under these conditions (Plattner *et al.*, 2006). No spill-over of calcium into somatic domains below the ciliary basis has been seen under standard stimulation conditions (Fig. 13). This may be due to the restricted open time of these channels, which are deactivated by the very same Ca^{2+} that they transport (Brehm and Eckert, 1978). In the opposite direction, spill-over of Ca^{2+} into cilia occurs during AED-stimulated exocytosis that then can also activate ciliary reversal in *Paramecium* mutants devoid of functioning Ca^{2+} channels in their cilia (Husser *et al.*, 2004; Plattner *et al.*, 1984). In conclusion, Ca^{2+} regulated ciliary activity is much more of the microdomain type, with calcium normally remaining in cilia as its target domain, than exo-endocytosis occurring in the somatic part of these cells. No comparable data are available from other ciliated cells.

Altogether cyclic nucleotides, notably cGMP, seem to play merely a modulatory role in ciliary activity, whereas that of Ca^{2+} appears much more essential (Nakaoka and Machemer, 1990). Although this view has not remained undisputed, our quenched-flow analyses have shown that in cilia, [Ca] and cAMP rise swiftly during depolarization and hyperpolarization, respectively, within one to two strokes (Fig. 13), while cGMP formation lags behind hyperpolarization (Yang *et al.*, 1997).

D. Rapid Coupling of Ca^{2+}-Influx with Cortical Stores

In some experiments with *Paramecium* $[Ca^{2+}]_o$ was reduced to $\sim 10^{-5}$ M, and $[Ca^{2+}]_o$ increased to 0.5 mM only in the depolarization medium (20 mM KCl) during quenched-flow/cryofixation, followed by EDX analysis (Plattner *et al.*, 2006). In that case, we expected a particularly strong [Ca] signal because of the high Ca^{2+} gradient. In fact, [Ca] values recorded exceeded signals achieved under any other conditions. [Ca] in cilia culminated at 80 ms (i.e., within two strokes) with some spill-over in the same time into the nearby cytosol. Moreover, unexpectedly this was accompanied by a very strong calcium signal in alveolar sacs, with a maximum between 80 and 100 ms after depolarization. In this cortical [Ca] store, [Ca] peak values exceeded 3× those measured in cilia. This rapid transient coupling between the extracellular space and the cortical compartment was very surprising, particularly considering the distant spatial arrangement of cilia and the [Ca] pools.

An even more rapid coupling between the extracellular space and the cortical compartment occurred during massive, synchronous exocytosis stimulation (Hardt and Plattner, 2000). Ca^{2+}/Sr^{2+} substitution during stimulation (see Section II.D) revealed very intense and rapid coupling of Ca^{2+} mobilization from cortical stores, with superimposed SOC, eventually visualized by Sr^{2+} (Hardt and Plattner, 2000; Fig. 9D–F).

Both these observations may be relevant with regard to ongoing discussions on the nature of this coupling, particularly during SOC-type reactions. For rapid coupling, physical linkage between the cortical stores and the cell membrane appeared mandatory to most investigators and a variety of structural proteins have been implied (Parekh and Putney, 2005; Randriamampita and Trautmann, 2004; Rosado *et al.*, 2005) including matching Ca^{2+} channels (Islam, 2003). To recall, in the case of ciliary reversal in *Paramecium* under over-stimulation conditions, Ca^{2+} is transferred from the outside medium via cilia to the cortical stores, so that no physical coupling can occur in that case. Rather, rapid cation exchange mechanisms may account for this unexpected phenomenon, particularly considering that refilling by the SERCA-type Ca^{2+}-pump is by orders of magnitude too sluggish (Mohamed *et al.*, 2003). This recalls the rapid cation counter-transport seen by cryofixation/EDX-analysis in the sarcoplasmic reticulum of skeletal muscle after tetanic stimulation (Somlyo *et al.*, 1981). Such a mechanism, when subsequently operating in the opposite direction, could lead to a rapid dissipation of Ca^{2+} into the nearby cytosol, as observed with *Paramecium*.

Although the SOC mechanism *per se* has been studied over the years (Lewis, 1999; Parekh and Penner, 1997; Parekh and Putney, 2005; Putney *et al.*, 2001; Randriamampita and Trautmann, 2004) some results appeared more in favor of a rather direct coupling mechanism (Islam, 2003; Rosado and Sage, 2000; Rosado *et al.*, 2005). Findings of rapid coupling between Ca^{2+} from the outside medium and in cortical stores under massive exocytosis stimulation and over-stimulated ciliary reversal, respectively, may have some general importance. In fact, such tight coupling is also discussed for many other cells, such as lymphocytes, based on widely different methodology (Narayanan *et al.*, 2003). Nevertheless, the data achieved during over-stimulated ciliary reversal indicate that tight physical linkage, not to speak of matching channels in the two membranes (the plasmamembrane and the cortical calcium store), cannot be the (only) explanation for rapid Ca^{2+} exchange to occur. Unfortunately functional properties of cortical Ca^{2+} stores, although being important in many cells, are not well understood. Additional details remain to be elucidated.

E. Additional Data on Intracellular Signaling

The method under consideration can retrieve additional biochemical/functional data. For instance, in *Paramecium* exo-endocytosis is accompanied by formation of cGMP (Knoll *et al.*, 1992a) and by rapid reversible dephosphorylation of a defined protein, pp63/parafusin (Höhne-Zell *et al.*, 1992). This occurs within 80 ms (Fig. 14), the time required for trichocyst exocytosis (Fig. 6). After cloning of its gene and its identification as phosphoglucomutase (Hauser *et al.*, 1997), a key-enzyme at the beginning of glycolysis,

the phenomenon described is understood as contributing to the re-establishment of ATP homeostasis after exocytosis (Müller *et al.*, 2002). This complex aspect is discussed in more detail elsewhere (Plattner and Kissmehl, 2005).

Another observation with *Paramecium* is that AED stimulation causes a rapid increase of [Ca] in cortically positioned mitochondria, followed by a rapid decrease, all within 1 s (Hardt and Plattner, 2000). Such rapid changes have only been reported from heart muscle mitochondria, where $[Ca^{2+}]$ oscillates with every beat (Robert *et al.*, 2001). This phenomenon does not occur during ciliary reversal induction, even when over-stimulated (Plattner *et al.*, 2006).

IV. Other Methodology

A. Correlation of Quenched-Flow/EM Analysis with Supplementary Methods

Principally widely different methods should be combined to elucidate complex dynamic events. For instance, in unstimulated *Paramecium* cells, ESI shows the selective enrichment of Ca signals in the alveolar sacs (Knoll *et al.*, 1993). According to cell fractionation and ATP-dependent $^{45}Ca^{2-}$ uptake measurements, alveolar sacs represent well-established subplasmalemmal Ca-stores (Stelly *et al.*, 1991; Länge *et al.*, 1995). (This function is not yet ascertained for similar structures occurring in closely related pathogenic members of the phylum Alveolata, including *Toxoplasma* and the malaria-causing agent, *Plasmodium*.) In ESI micrographs obtained 80 ms after AED stimulation, some Ca signal still resides in alveolar sacs, but in addition strong signals become apparent all along the plasmamembrane (Knoll *et al.*, 1993) (Fig. 7). Because alveolar sacs are attached parallel to the plasmamembrane with a distance of only 15 nm, only the spatial resolution of ESI (but not that of EDX, as discussed later) suffices to differentiate between Ca signals originating from stores or from the subplasmalemmal space. The plasmamembrane-bound ESI signals are equivalent to the Ca^{2-} that activates the different Ca^{2-}-dependent ion currents occurring throughout the cell membrane during different types of stimulation (Machemer, 1988; Preston and Saimi, 1990). In agreement with Ca-imaging by ESI, such currents can be registered during AED stimulated exocytosis (Erxleben and Plattner, 1994; Erxleben *et al.*, 1997). Moreover, [Ca] imaging by ESI (Fig. 7) or EDX (Fig. 9) reveals rather equal distribution of calcium within alveolar sacs—in agreement with the rapid Ca^{2} equilibration in stores, as observed with other methods (Park *et al.*, 2000).

To what extent can data from so widely different methods, such as electrophysiology, fluorochrome analysis and analytical EM, be correlated? In *Paramecium*, the minimal electrical currents accompanying single exocytotic events had a half-width of $t_{1/2} = 21$ ms (Erxleben *et al.*, 1997). This is well within the time range of exocytosis performance which operates with $t_{1/2} = 56$ ms for all events (Plattner *et al.*, 1992). This is also well compatible with the Ca^{2+} sparks registered with fluorochrome-injected cells during AED stimulation at low $[Ca^{2+}]_o$ (precluding Ca^{2+} influx). For this, a fast confocal laser scanning microscope, CLSM, equipped with an optoacoustic beam deflection system allowing image collection in ~30 ms intervals, has been used (Klauke *et al.*, 2000). Ca^{2+} sparks show up only from one image to another. In summary, quenched-flow/EDX, electrophysiology, and CLSM are all compatible within about the same time scale.

Considering that optical methods record $[Ca^{2+}]$, while ESI and EDX register [Ca] (i.e., free Ca^{2+} and structure-bound calcium), comparison of both components should allow to estimate total Ca^{2+} fluxes, to yield $[Ca^{2+}]_i^{act}$ for activation of exocytosis and ensuing endocytosis. Additional information comes from injection of calcium buffers of different affinity (K_d) immediately followed by AED stimulation. Thus, we determined that a local $[Ca^{2+}]_i^{act}$ of ~5 μM is required to induce exocytosis (Plattner and Klauke, 2001). This is ~10× higher than registered by fluorochromes in the cell cortex during AED stimulation (Klauke and Plattner, 1997)—a phenomenon which is well known from other cells (Marengo and Monck, 2000; Neher, 1998). Much higher $[Ca^{2+}]$ values would be expected from both, $^{45}Ca^{2+}$ influx measurements during AED stimulation, combined with quenched-flow analysis (Knoll *et al.*, 1992a), and from the measured release from alveolar sacs (Hardt and Plattner, 2000). Generally such discrepancies can be explained by rapid sequestration and extrusion, and in particular by binding to cytosolic Ca^{2+}-binding proteins (Neher, 1998; Pozzo-Miller *et al.*, 1999; Thomas *et al.*, 1993). The latter component may preponderate in *Paramecium* where reuptake into (cortical) stores by the Ca^{2+}-pump is rather slow (Mohamed *et al.*, 2003).

From all this, the following questions then arise. To what extent is $[Ca^{2+}]_i^{act}$ generated by mobilization from alveolar sacs? Which proportion is due to Ca^{2+} influx? What may be the causative interaction between the two phenomena? What are the total Ca^{2+} fluxes during stimulation? Clearly only a combination of different methods appears appropriate to address these questions. Again EDX in combination with quenched-flow and freeze-substitution under conditions of Ca retention is the method of choice.

The approach involved stimulating cells with AED after rapid adjustment of $[Ca^{2+}]_o$ to different levels, from 30 nM to >1 mM, combined with quenched-flow/freeze-fracture preparation (Knoll *et al.*, 1993; Plattner *et al.*, 1997) (Fig. 11). AED stimulation under conditions when $[Ca^{2+}]_o < [Ca^{2+}]_i^{rest}$ still results in some exocytosis, thus indicating the relevance of

internal release as one signaling component. Because all steps of the exo-endocytotic cycle are accelerated by increased $[Ca^{2+}]_o$ (Plattner *et al.*, 1997), exocytosis must normally involve additional Ca^{2+} supply from influx. Not only fluorochrome analyses (Klauke *et al.*, 2000), but also EDX studies (Hardt and Plattner, 2000; Mohamed *et al.*, 2002) revealed that AED stimulated exo-endocytosis involves a SOC. This implies that Ca^{2+} is first mobilized from alveolar sacs and that the empty signal causes an influx of Ca^{2+} from the medium. Although this is a widely distributed signaling mechanism (Lewis, 1999; Parekh and Penner, 1997; Putney *et al.*, 2001), a combined methodology can elucidate more details. In fact, when *Paramecium* cells are stimulated by AED very shortly after rapid Sr^{2+}/Ca^{2+} exchange in the medium (all executed during the quenched-flow procedure), Sr appears in alveolar sacs very rapidly (Hardt and Plattner, 2000), thus supporting a SOC-type mechanism (see Fig. 9 and Section III.D). Despite this, during exocytosis stimulation, over a period of 1 s, [Ca] in alveolar sacs rapidly decreases to about half of its original value (Fig. 9C). This decrease is independent of a Ca^{2+}- influx—as to be expected for a SOC-type mechanism—because it occurs also with mutants devoid of any stimulated Ca^{2+}-influx (Mohamed *et al.*, 2002) (Fig. 10). Thus, the methodology under consideration allows one to dissect a very complicated interplay between (1) Ca^{2+} mobilization from cortical stores, (2) Ca^{2+}-influx (including stores), and (3) ongoing Ca^{2+} release.

There are, however, aspects in favor of some alternative techniques. For instance, the most crucial step of exocytosis, membrane fusion, is $\sim 10\times$ faster and smaller than the resolution of 10 nm and ~ 1 ms available by the cryofixation/EM analysis, what one can see on freeze-fracture replicas of stimulated cells. Electrophysiology, that is patch-clamp analysis, would be considerably superior because it is able to show (in other systems) that individual fusion events are much faster, particularly with small, clear (neurotransmitter) vesicles. From the conductivity of pores determined by patch-clamp analysis one could derive the formation molecular-sized pores (Almers, 1990) before they enlarge to a size visible in the EM. On the other hand, electrophysiological analyses cannot determine any other structural detail characteristic of membrane fusion, like rosettes in *Paramecium* and their decay into subunits. Furthermore, for many years endocytotic membrane resealing was not amenable to patch-clamp analysis (Rosenboom and Lindau, 1994), whereas quenched-flow/freeze-fracturing allowed the determination even of the kinetics of ghost internalization (Plattner *et al.*, 1997). Both methods have shown that the entire exo-endocytic cycle is sped up by increasing $[Ca^{2+}]_o$.

With regard to total Ca^{2+} movements during exo-endocytosis, both electrophysiology with other secretory systems (Pozzo-Miller *et al.*, 1999; Thomas *et al.*, 1993) and analyses with *Paramecium* (Hardt and Plattner, 2000; Plattner

and Klauke, 2001) have shown that a cell operates with a tremendous excess of Ca^{2+} to achieve ~10 μM at the strategic sites of membrane fusion and detachment. This has to be expected from the rapid $[Ca^{2+}]_i$ down-regulation known to occur in the cytosol.

Such correlations are more difficult to achieve with ciliary beat regulation although this process has been thoroughly analyzed by alternative methods already. *In vitro* studies with permeabilized *Paramecium* cells have revealed that the ciliary beat is reversed at $[Ca^{2+}] > 10^{-6}$ M (Naitoh and Kaneko, 1972; Tamm, 1994), as it would occur *in vivo* during depolarization-induced Ca^{2+}-influx via voltage-dependent Ca^{2+}-channels (Eckert and Brehm, 1979). With intact cells, analysis of $[Ca^{2+}]$ dynamics in cilia with fluorochromes is problematic (Pernberg and Machemer, 1995; Tamm and Terasaki, 1994) and recording along the extension of a cilium is literally impossible. Quenched-flow/cryofixation/EDX analysis after 80 ms depolarization allowed us to demonstrate a rather uniform [Ca] increase along some extension of individual cilia (Husser *et al.*, 2004; Plattner *et al.*, 2006) (Fig. 13). This correlates with the probably uniform distribution of Ca^{2+} targets along the extension of a cilium or a flagellum (Casey *et al.*, 2003; Kim *et al.*, 2002), and it may reflect an even distribution of Ca^{2+}-influx channels (which have not been localized with any precision within the ciliary membrane). In *Paramecium* cells, this overall localization holds for the protein phosphatase, PP2C (Grothe *et al.*, 1998), which is considered crucial for regulating cAMP-dependent ciliary beat control (Noguchi *et al.*, 2003). In *Chlamydomonas*, this serves to detach outer dynein arms from peripheral microtubules during the flagellar beat (Sakato and King, 2003).

As shown in Fig. 13, hardly any spill-over into somatic domains is seen during depolarization under standard stimulation conditions (Husser *et al.*, 2004), which may be attributed to rapid binding to intraciliary proteins (i.e., effective buffering) and to the closing of these channels by the intraciliary $[Ca^{2+}]_i$ increase (Brehm and Eckert, 1978). On the other hand, after AED stimulation, the same methodology shows that a Ca^{2+} spill-over from the cell cortex into cilia does occur (Husser *et al.*, 2004), thus explaining the occurrence of ciliary reversal in mutants devoid of Ca^{2+}-influx channels (Plattner *et al.*, 1984). Moreover, spill-over from cilia into alveolar sacs and into the adjacent cytosol occurs when ciliary reversal is over-stimulated by an unusually high $[Ca^{2+}]_o/[Ca^{2+}]_i$ gradient during depolarization (Plattner *et al.*, 2006). In sum, combined methodologies can yield clues to possible pathways of intracellular cross-talk.

In *Paramecium*, the ciliary beat during hyperpolarization or depolarization is also regulated by cyclic nucleotides (Hamasaki *et al.*, 1991; Majima *et al.*, 1986; Nakaoka and Machemer, 1990; Pech, 1995; Preston and Saimi, 1990; Schultz and Klumpp, 1993). A precise time correlation, eventually in addition to published video recordings, was possible by the use of quenched-flow

analysis. Upon hyperpolarization, cAMP increases several times within one ciliary stroke, while depolarization-induced cGMP formation lags behind (Yang *et al.*, 1997). Because the latter depends on a $[Ca^{2+}]$ increase (Schultz and Klumpp, 1993) this could also explain the increase of cGMP during AED-stimulated exocytosis (Knoll *et al.*, 1992a).

B. Complementary Light Microscopic and Other Techniques for Analyzing Fast Processes

Very fast subcellular processes down to the submillisecond time range require the fastest techniques available, such as electrophysiology including patch-clamp analysis (see Section II.A and III.A). For instance, exocytosis encompasses steps of widely different time constants (Jahn *et al.*, 2003), from extremely fast membrane fusion, followed by contents release within a time from < 1 s to several seconds, and finally endocytotic membrane resealing. For *Paramecium* cells, see Fig. 5. Specifically with chromaffin cells, release of catecholamines can be measured by amperometry for which electrodes have been continuously miniaturized. With a rather long delay, exocytosis-coupled endocytosis has become amenable to patch-clamp analysis. Besides space resolution in the sense of pore size estimation from conductivity during membrane fusion, there is no spatial resolution in the sense of correlation with structural detail of a cell. Recently, however, some spatial resolution has been achieved by using regularly spaced electrochemical detector arrays on microscope slides (Hafez *et al.*, 2005). Such microdetection arrays may allow for some spatial resolution in the future, thus complementing the unsurpassed time resolution achieved by patch-clamp analysis.

Spatial and temporal resolution of innovative light microscopic techniques has been improved with breathtaking speed. The progress encompasses new instrumentation exploiting novel imaging principles. Also, novel labeling techniques, including molecularly tailored fluorescent markers, have been developed. Thus in principle, real time analyses have become possible on the level of single molecules. A closer look shows, however, that such techniques will hardly replace the technologies that are the focus of this review. Rather they complement the ever-growing methodical repertoire, thus addressing a spectrum of additional, refined questions in cell biological research. This can be discussed only briefly in the present context.

Some of the numerous new light microscopic techniques try to reduce the limitations of spatial resolution, as exemplified by the work of Hell *et al.* (2004), even in thick samples (Huisken *et al.*, 2004). This goal is also followed up by the CLSM technology (Yuste, 2005). Temporal resolution of CLSM has been considerably improved already some time ago by using rapid beam deflection systems, eventually combined with rapid ratio imaging (e.g., of

ion-specific fluorochromes). An example related to EDX/EM analyses discussed in this review is the work by Brochet *et al.* (2005).

Fluorescence de-quenching, using labeled lipid vesicles or biomembranes, is another longstanding method to study membrane fusion. For example, fusion mediated by SNARE proteins has thus been analyzed (Fix *et al.*, 2004). In another approach, the amphipathic styrene dye, FM1-43, is allowed to become incorporated into the cell membrane (Betz *et al.*, 1992). As a consequence of membrane fusion during exocytosis stimulation, the dye diffuses into secretory vesicle membranes from where it can be released after recycling and a second round of exocytosis. Richards *et al.* (2005) present an example dealing with synaptic vesicle trafficking in brain cells; such analyses did not aim specifically at high resolution, though.

The numerous fluorescent protein tags now available, such as green/yellow/cyano/red fluorescent proteins (e.g., GFP), provide a new handle to study subcellular dynamics (Lippincott-Schwartz and Patterson, 2003; Miyawaki *et al.*, 2003; Tsien, 2005). Most work along these lines covers a much larger time scale than addressed in the present review. These light microscopic developments can be very powerful, such as when combined with total internal reflection (evanescent wave) microscopy or fluorescence resonance energy transfer (FRET), (see Stephens and Allan, 2003; Toomre and Manstein, 2001). Using fluorescent liposomes for *in vitro* experiments, sufficient time resolution has been achieved when the liposomes and a planar lipid layer, respectively, have been reconstituted with SNARE proteins for fusion analysis by total internal reflection microscopy within a time range of <25 ms (Liu *et al.*, 2005). Spatial resolution in the context of FRET is ambiguous. FRET requires molecules to approach each other within <3 nm, but assignment to structural details of a cell is restricted. Nevertheless, FRET techniques have become important tools to analyze local interactions of molecules, also in the sub-second time range. Examples are cells transfected with constructs that encode a combination of a Ca^{2+}-sensitive protein capable of undergoing a conformational change upon activation (binding of Ca^{2+}), such as calmodulin, and of a target molecule, so they get close enough to each other (Rudolf *et al.*, 2004; Tsien, 2005). An ever-expanding number of fluorescent proteins are becoming available (Yang *et al.*, 2005). This may allow further expansion of this important innovation.

With regard to Ca^{2+} imaging, new light microscopic technologies give us a useful time range. This is above that covered by electrophysiology, but below that available for the analysis of total calcium concentrations by quenched-flow/cryofixation combined with EDX (see Section II.B and D). It should be noted that the time constants of the Ca^{2+}-fluorochromes available are small enough (Neher, 1995, 1998; see also Plattner and Klauke, 2001) to be exploited by the available improved instrumentation. In the end, it would be desirable to determine calcium concentrations, [Ca] and [Ca^{2+}] respectively,

with the highest possible spatial and temporal resolution. This postulate results from the (Ca^{2+}-dependent) co-assembly of molecular partners in microdomains (e.g., at exocytosis sites) (Ambudkar, 2006; Barclay *et al.*, 2005; Rizzuto and Pozzan, 2006; Rosado *et al.*, 2005), the rapid binding to endogenous molecules interacting with one another in a Ca^{2+}-dependent manner (Bai *et al.*, 2004), and the involvement of only a few Ca^{2+} molecules to achieve the local $[Ca^{2+}]_i$ required for a local response (Schneggenburger and Neher, 2005). Among structural methods, a useful approach is to register Ca^{2+} sparks during local activation under restrictive conditions, such as by quenching $[Ca^{2+}]_i$ responses by intracellular application of Ca^{2+} buffers with known binding constant (Neher, 1995, 1998), or by reducing Ca^{2+}-influx, to determine threshold values required to abolish the response under consideration. Both methods have been successfully applied also to *Paramecium* (Klauke and Plattner, 1997; Klauke *et al.*, 2000).

Beyond Ca^{2+}-imaging, an increasing number of fluorochromes became available on the market, including some for different ions, pH, membrane potential, etc. (Lichtman and Concello, 2005). Other work in the sub-second time range combines uncaging of "caged" compounds (Politz, 1999), such as Ca^{2+}, inositol 1,4,5-trisphosphate, cyclic nucleotides, and some other second messengers (Lee, 2005). This can be applied in conjunction with fluorescent imaging of various signals or with widely different technologies. An example is the analysis of the flagellar beat in sea urchin sperm during chemotaxis in dependency of cyclic 3′,5′-GMP formation and $[Ca^{2+}]_i$ increase (Böhmer *et al.*, 2005; Wood *et al.*, 2005). Eventually such analyses have been performed with the help of quenched-flow techniques (Matsumoto *et al.*, 2003). Already, uncaging of ATP has been combined with timed cryofixation to analyze actin/myosin interaction in EM (Hirose *et al.*, 1993). Unfortunately such powerful technical combinations have not been followed up.

V. Concluding Remarks

Despite a multitude of very useful new developments in light microscopy and some additional technologies, there still is ample space for the application of EM methodologies to the study of subcellular dynamics. Beyond the examples discussed in this review, EM techniques proved most appropriate for unraveling the intriguing dynamics of the Golgi apparatus (Koster and Klumperman, 2004) and for establishing the existence of microdomains, with partners co-assembled in part on the outer, and in part on the inner side of a membrane (Stuermer *et al.*, 2004), to give just some examples. It would also be most interesting to see the powerful technique of electron tomography of cryofixed cells (Lucic *et al.*, 2005) expanded to dynamic

events. Though not necessarily very demanding with regard to time resolution, questions of this kind are frequently difficult to analyze by any other technique. This review presents a variety of examples in which time-resolved data can reasonably be combined with EM analysis.

Lack of time resolution of the EM instrument can be overcome by time-resolved preparation protocols, involving cryofixation at different times during synchronous stimulation of dynamic events combined with quenched-flow. Examples are exocytosis and endocytosis as well as ciliary beat activity. For structural analyses of very rapid events in biomembranes, freeze-fracture can be used as a follow-up procedure. Analytical capabilities of the EM can be exploited (e.g., by ESI or EDX), provided elements to be analyzed can be retained. One can then follow quantitatively the distribution of total [Ca] during stimulation, such as within stores and near activation sites. All this can be performed in the sub-second time range. The data thus obtained can be compared with widely different alternative methods (e.g., with $[Ca^{2-}]$ recordings). Moreover, the dynamics of other second messengers, such as cAMP or cGMP, can be followed, the regulation of ciliary activity being an example. An increasing number of complementary methods, in widely varied combinations, will allow us to address an increasing multiplicity of problems in cell biology. One of the persisting aims will be to increase temporal and spatial resolution.

Acknowledgments

We gratefully acknowledge the financial support of the author's work cited herein by grants from the Deutsche Forschungsgemeinschaft.

References

Abelson, J., Simon, M., and Marriott, G. (1998). "Caged Compounds." Academic Press, New York.

Ales, E., Tabares, L., Poyato, J. M., Valero, V., Lindau, M., and Alvarez De Toledo, G. (1999). High calcium concentrations shift the mode of exocytosis to the kiss-and-run mechanism. *Nature Cell Biol.* **1**, 40–44.

Almers, W. (1990). Exocytosis. *Annu. Rev. Physiol.* **52**, 607–624.

Ambudkar, I. S. (2006). Ca^{2+} signaling microdomains: Platforms for the assembly and regulation of TRPC channels. *Trends Pharmacol. Sci.* **27**, 25–32.

Bachmann, L., and Schmidt, W. W. (1971). Improved cryofixation applicable to freeze-etching. *Proc. Natl. Acad. Sci. USA* **68**, 2149–2152.

Bai, J., Wang, C.-T., Richards, D. A., Jackson, M. B., and Chapman, E. R. (2004). Fusion pore dynamics are regulated by synaptotagmin. t-SNARE interactions. *Neuron* **41**, 929–942.

Barclay, J. W., Morgan, A., and Burgoyne, R. D. (2005). Calcium-dependent regulation of exocytosis. *Cell Calcium* **38**, 343–353.

Bauer, R. (1988). Electron spectroscopic imaging: An advanced technique for imaging and analysis in transmission electron microscopy. *Meth. Microbiol.* **20,** 113–146.

Berridge, M. J. (1998). Neuronal calcium signaling. *Neuron* **21,** 13–26.

Berridge, M. J., Lipp, P., and Bootman, M. D. (2000). The calcium entry pas de deux. *Science* **287,** 1604–1605.

Berridge, M. J., Bootman, M. D., and Roderick, H. L. (2003). Calcium signalling: Dynamics, homeostasis and remodelling. *Nature Rev. Mol. Cell Biol.* **4,** 517–529.

Berriman, J., and Unwin, N. (1994). Analysis of transient structures by cryo-microscopy combined with rapid mixing of spray droplets. *Ultramicroscopy* **56,** 241–252.

Bers, D. M., Patton, C. W., and Nuccitelli, R. (1994). A practical guide to the preparation of Ca^{2-} buffers. *Meth. Cell Biol.* **40,** 3–29.

Betz, W. B., Mao, F., and Bewick, G. S. (1992). Activity-dependent fluorescent staining and destaining of living motor nerve terminals. *J. Neurosci.* **12,** 363–375.

Böhmer, M., Van, Q., Weyand, I., Hagen, V., Beyermann, M., Matsumoto, M., Hoshi, M., Hildebrand, E., and Kaupp, U. B. (2005). Ca^{2-} spikes in the flagellum control chemotactic behavior of sperm. *EMBO J.* **24,** 2741–2752.

Brehm, P., and Eckert, R. (1978). Calcium entry leads to inactivation of calcium channel in *Paramecium*. *Science* **202,** 1203–1206.

Brochet, D. X. P., Yang, D., Di Maio, A., Lederer, W. J., Franzini-Armstrong, C., and Cheng, H. (2005). Ca^{2-} blinks: Rapid nanoscopic store calcium signaling. *Proc. Natl. Acad. Sci. USA* **102,** 3099–3104.

Burgoyne, R. D., Fisher, R. J., Graham, M. E., Haynes, L. P., and Morgan, A. (2001). Control of membrane fusion dynamics during regulated exocytosis. *Biochem. Soc. Trans.* **29,** 467–472.

Casey, D. M., Yagi, T., Kamiya, R., and Witman, G. B. (2003). DC3, the smallest subunit of the *Chlamydomonas* flagellar outer dynein arm-docking complex, is a redox-sensitive calcium-binding protein. *J. Biol. Chem.* **278,** 42652-42659.

Cheek, T. R., Murawsky, M. M., and Stauderman, K. A. (1994). Histamine-induced Ca^{2} entry precedes Ca^{2+} mobilization in bovine adrenal chromaffin cells. *Biochem. J.* **304,** 469–476.

Cherepanov, A. V., and DeVries, S. (2004). Microsecond freeze-hyperquenching: Development of a new ultrafast micro-mixing and sampling technology and application to enzyme catalysis. *Biochim. Biophys. Acta* **1656,** 1–31.

Chestnut, M. H., Siegel, D. P., Burns, J. L., and Talmon, Y. (1992). A temperature-jump device for time-resolved cryo-transmission electron microscopy. *Microsc. Res. Techn.* **20,** 95–101.

Chow, R. H., von Rüden, L., and Neher, E. (1992). Delay in vesicle fusion revealed by electrochemical monitoring of single secretory events in adrenal chromaffin cells. *Nature* **356,** 60–63.

Conner, S. D., and Schmid, S. L. (2003). Regulated portals of entry into the cell. *Nature* **422,** 37–44.

Dernick, G., Gong, L.-W., Tabares, L., Alvarez de Toledo, G., and Lindau, M. (2005). Patch amperometry: High-resolution measurements of single-vesicle fusion and release. *Nature Meth.* **2,** 699–708.

Dunford, H. B. (1983). Stopped-flow, temperature-jump and flash photolysis techniques: Effect of temperature, dielectric constant and viscosity. *In* "Fast Methods in Physical Biochemistry and Cell Biology" (R. I. Sha'afi and S. M. Fernandez, Eds.), pp. 11–38. Elsevier Science, Amsterdam.

Eckert, R., and Brehm, P. (1979). Ionic mechanisms of excitation in *Paramecium*. *Annu. Rev. Biophys. Bioeng.* **8,** 353–383.

Erxleben, C., and Plattner, H. (1994). Ca^{2-} release from subplasmalemmal stores as a primary event during exocytosis in *Paramecium* cells. *J. Cell Biol.* **127,** 935–945.

Erxleben, C., Klauke, N., Flötenmeyer, M., Blanchard, M.-P., Braun, C., and Plattner, H. (1997). Microdomain Ca^{2-} activation during exocytosis in *Paramecium* cells. Superposition of local subplasmalemmal calcium store activation by local Ca^{2-} influx. *J. Cell Biol.* **136,** 597–607.

Eskandari, S., Wright, E. M., Kreman, M., Starace, D. M., and Zampighi, G. A. (1998). Structural analysis of cloned plasma membrane proteins by freeze-fracture electron microscopy. *Proc. Natl. Acad. Sci. USA* **95,** 11235–11240.

Fix, M., Malia, T. J., Jaiswal, J. K., Rappoport, J. Z., You, D., Söllner, T. H., Rothman, J. E., and Simon, S. M. (2004). Imaging single membrane fusion events mediated by SNARE proteins. *Proc. Natl. Acad. Sci. USA* **101,** 7311–7316.

Froissard, M., Kissmehl, R., Dedieu, J.-C., Gulik-Krzywicki, T., Plattner, H., and Cohen, J. (2002). N-ethylmaleimide-sensitive factor is required to organize functional exocytotic microdomains in *Paramecium*. *Genetics* **161,** 643–650.

Gandhi, S. P., and Stevens, C. F. (2003). Three modes of synaptic vesicular recycling revealed by single-vesicle imaging. *Nature* **423,** 607–613.

Genazzani, A. A., Mezna, M., Summerhill, R. J., Galione, A., and Michelangeli, F. (1997). Kinetic properties of nicotinic acid adenine dinucleotide phosphate-induced Ca^{2+} release. *J. Biol. Chem.* **272,** 7669–7675.

Gore, M. G. (Ed.) (2000). "Spectrophotometry and Spectrofluorimetry. A Practical Approach." Oxford University Press, Oxford.

Grothe, K., Hanke, C., Momayezi, M., Kissmehl, R., Plattner, H., and Schultz, J. E. (1998). Functional characterization and localization of protein phosphatase type 2C from *Paramecium*. *J. Biol. Chem.* **273,** 19167–19172.

Gurunathan, S., Marash, M., Weinberger, A., and Gerst, J. E. (2002). t-SNARE phosphorylation regulates endocytosis in yeast. *Mol. Biol. Cell* **13,** 1594–1607.

Gutfreund, H. (1999). Rapid-flow techniques and their contributions to enzymology. *Trends Biochem. Sci.* **24,** 457–460.

Hafez, I., Kisler, K., Berberian, K., Dernick, G., Valero, V., Yong, M. G., Craighead, H. G., and Lindau, M. (2005). Electrochemical imaging of fusion pore openings by electrochemical detector arrays. *Proc. Natl. Acad. Sci. USA* **102,** 13879–13884.

Hamasaki, T., Barkalow, K., Richmond, J., and Satir, P. (1991). cAMP-stimulated phosphorylation of an axonemal polypeptide that copurifies with the 22S dynein arm regulates microtubule translocation velocity and swimming speed in *Paramecium*. *Proc. Natl. Acad. Sci. USA* **88,** 7918–7922.

Han, X., Wang, C.-T., Bai, J., Chapman, E. R., and Jackson, M. B. (2004). Transmembrane segments of syntaxin line the fusion pore of Ca^{2+}-triggered exocytosis. *Science* **304,** 289–292.

Hardt, M., and Plattner, H. (1999). Quantitative energy-dispersive X-ray microanalysis of calcium dynamics in cell suspensions during stimulation on a subsecond time scale: Preparative and analytical aspects as exemplified with *Paramecium* cells. *J. Struct. Biol.* **128,** 187–199.

Hardt, M., and Plattner, H. (2000). Sub-second quenched-flow/X-ray microanalysis shows rapid Ca^{2+} mobilization from cortical stores paralleled by Ca^{2+} influx during synchronous exocytosis in *Paramecium* cells. *Eur. J. Cell Biol.* **79,** 642–652.

Hauser, K., Kissmehl, R., Linder, J., Schultz, J. E., Lottspeich, F., and Plattner, H. (1997). Identification of isoforms of the exocytosis-sensitive phosphoprotein PP63 parafusin in *Paramecium tetraurelia* and demonstration of phosphoglucomutase activity. *Biochem. J.* **323,** 289–296.

Hell, S. W., Dyba, M., and Jakobs, S. (2004). Concepts for nanoscale resolution in fluorescence microscopy. *Curr. Op. Neurobiol.* **14,** 599–609.

Henkel, A. W., and Almers, W. (1996). Fast steps in exocytosis and endocytosis studied by capacitance measurements in endocrine cells. *Curr. Op. Neurobiol.* **6,** 350–357.

Henkel, A. W., Horstmann, H., and Henkel, M. K. (2001). Direct observation of membrane retrieval in chromaffin cells by capacitance measurements. *FEBS Lett.* **505,** 414–418.

Hess, G. P. (1993). Determination of the chemical mechanism of neurotransmitter receptor-mediated reactions by rapid chemical kinetic techniques. *Biochemistry* **32,** 989–1000.

Heuser, J. E., Reese, T. S., Dennis, M. J., Jan, Y., Jan, L., and Evens, L. (1979). Synaptic vesicle exocytosis captured by quick-freezing and correlated with quantal transmitter release. *J. Cell Biol.* **81,** 275–300.

Hiesinger, P. R., Fayyazuddin, A., Mehta, S. Q., Rosenmund, T., Schulze, K. L., Zhai, R. G., Verstreken, P., Cao, Y., Zhou, Y., Kunz, J., and Bellen, H. J. (2005). The v-ATPase V_0 subunit a1 is required for a late step in synaptic vesicle exocytosis in *Drosophila*. *Cell* **121,** 607–620.

Hirose, K., Lenart, T. D., Murray, J. M., Franzini-Armstron, C., and Goldman, Y. E. (1993). Flash and smash: Rapid freezing of muscle fibers activated by photolysis of caged ATP. *Biophys. J.* **65,** 397–408.

Höhne-Zell, B., Knoll, G., Riedel-Gras, U., Hofer, W., and Plattner, H. (1992). A cortical phosphoprotein ('PP63') sensitive to exocytosis triggering in *Paramecium* cells. Immunolocalization and quenched-flow correlation of time course of dephosphorylation with membrane fusion. *Biochem. J.* **286,** 843–849.

Huisken, J., Swoger, J., Del Bene, F., Wittbrodt, J., and Stelzer, E. H. (2004). Optical sectioning deep inside live embryos by selective plane illumination microscopy. *Science* **305,** 1007–1009.

Husser, M. R., Hardt, M., Blanchard, M.-P., Hentschel, J., Klauke, N., and Plattner, H. (2004). One-way calcium spill-over during signal transduction in *Paramecium* cells: From the cell cortex into cilia, but not in the reverse direction. *Cell Calcium* **36,** 349–358.

Ingram, P., Shelburne, J. D., and Lefurgey, A. (1999). Principles and instrumentation. *In* "Biomedical Applications of Microprobe Analysis" (P. Ingram, J. D. Shelburne, V. L. Roggli, and A. Lefurgey, Eds.), pp. 1–57. Academic Press, San Diego, London, Boston.

Islam, M. N. (2003). Further evidence of a direct ER uptake model for capacitative calcium entry. *FASEB J.* **17,** A42–A43.

Jahn, R., and Südhof, T. C. (1999). Membrane fusion and exocytosis. *Annu. Rev. Biochem.* **68,** 863–911.

Jahn, R., Lang, T., and Südhof, T. C. (2003). Membrane fusion. *Cell* **112,** 519–533.

Jorgensen, A. O., Broderick, R., Somlyo, A. P., and Somlyo, A. V. (1988). Two structurally distinct calcium storage sites in rat cardiac sarcoplasmic reticulum: An electron microprobe analysis study. *Circ. Res.* **63,** 1060–1069.

Kasai, H. (1999). Comparative biology of Ca^{2+}-dependent exocytosis: Implications of kinetic diversity for secretory function. *Trends Neurosci.* **22,** 88–93.

Kavalali, E. T., Klingauf, J., and Tsien, R. W. (1999). Properties of fast endocytosis at hippocampal synapses. *Phil. Trans. R. Soc. London B* **354,** 337–346.

Kerboeuf, D., and Cohen, J. (1990). A Ca^{2+} influx associated with exocytosis is specifically abolished in a *Paramecium* exocytotic mutant. *J. Cell Biol.* **111,** 2527–2535.

Kim, K., Son, M., Peterson, J. B., and Nelson, D. L. (2002). Ca^{2+}-binding proteins of cilia and infraciliary lattice of *Paramecium tetraurelia*: Their phosphorylation by purified endogenous Ca^{2+}-dependent protein kinases. *J. Cell Sci.* **115,** 1973–1984.

Kissmehl, R., Froissard, M., Plattner, H., Momayezi, M., and Cohen, J. (2002). NSF regulates membrane traffic along multiple pathways in *Paramecium*. *J. Cell Sci.* **115,** 3935–3946.

Kissmehl, R., Wassmer, T., Danzer, C., Nuehse, K., Lutter, K., Schilde, C., and H., Plattner Molecular identification of 26 syntaxin genes and their assignment to the different trafficking pathways in *Paramecium*, in press.

Klauke, N., and Plattner, H. (1997). Imaging of Ca^{2+} transients induced in *Paramecium* cells by a polyamine secretagogue. *J. Cell Sci.* **110,** 975–983.

Klauke, N., Blanchard, M.-P., and Plattner, H. (2000). Polyamine triggering of exocytosis in *Paramecium* involves an extracellular Ca^{2+} (polyvalent cation)-sensing receptor, subplasmalemmal Ca-store mobilization and store-operated Ca^{2+} influx via unspecific cation channels. *J. Membr. Biol.* **174,** 141–156.

Knipper, M., Beck, A., Rylett, J., and Breer, H. (1993). Neutrophin induced cAMP and IP_3 responses in PC12 cells. Different pathways. *FEBS Lett.* **324,** 147–152.

Knoll, G., Grässle, A., Braun, C., Probst, W., Höhne-Zell, B., and Plattner, H. (1993). A calcium influx is neither strictly associated with nor necessary for exocytotic membrane fusion in *Paramecium* cells. *Cell Calcium* **14,** 173–183.

Knoll, G., Kerboeuf, D., and Plattner, H. (1992a). A rapid calcium influx during exocytosis in *Paramecium* cells is followed by a rise in cyclic GMP within 1s. *FEBS Lett.* **304,** 265–268.

Knoll, G., Plattner, H., and Nordmann, J. J. (1992b). Exo-endocytosis in isolated peptidergic nerve terminals occurs in the sub-second range. *Biosci. Rep.* **12,** 495–501.

Knoll, G., Braun, C., and Plattner, H. (1991). Quenched flow analysis of exocytosis in *Paramecium* cells: Time course, changes in membrane structure and calcium requirements revealed after rapid mixing and rapid freezing of intact cells. *J. Cell Biol.* **113,** 1295–1304.

Koster, A. J., and Klumperman, J. (2004). Electron microscopy in cell biology: Integrating structure and function. *Nature Rev. Microsc. Coll.* **2004,** 31–35.

Krupa, B., and Liu, G. (2004). Does the fusion pore contribute to synaptic plasticity? *Trends Neurosci.* **27,** 62–66.

Kumar, R., Prabhu, N. P., and Bhuyan, A. K. (2005). Ultrafast events in the folding of ferrocytochrome c. *Biochemistry* **44,** 9359–9367.

Lang, R. D. A., and Bronk, J. R. (1978). A study of rapid mitochondrial structural changes in vitro by spray-freeze-etching. *J. Cell Biol.* **77,** 134–147.

Länge, S., Klauke, N., and Plattner, H. (1995). Subplasmalemmal Ca^{2+} stores of probable relevance for exocytosis in *Paramecium*. Alveolar sacs share some but not all characteristics with sarcoplasmic reticulum. *Cell Calcium* **17,** 335–344.

Lee, H. (2005). Nicotinic acid adenine dinucleotide phosphate (NAADP)-mediated calcium signaling. *J. Biol. Chem.* **280,** 33693–33696.

Lewis, R. S. (1999). Store-operated calcium channels. *Adv. Sec. Mess. Phosphoprot. Res.* **33,** 279–307.

Lichtman, J. W., and Conchello, J.-A. (2005). Fluorescence microscopy. *Nature Meth.* **2,** 910–919.

Lippincott-Schwartz, J., and Patterson, G. H. (2003). Development and use of fluorescent protein markers in living cells. *Science* **300,** 87–91.

Liu, T., Tucker, W. C., Bhalla, A., Chapman, E. R., and Weisshaar, J. C. (2005). SNARE-driven, 25-millisecond vesicle fusion *in vitro*. *Biophys. J.* **89,** 2458–2472.

Lucic, V., Forster, F., and Baumeister, W. (2005). Structural studies by electron tomography: From cells to molecules. *Annu. Rev. Biochem.* **74,** 833–865.

Machemer, H. (1988). Electrophysiology. *In* "Paramecium" (H.-D Görtz, Ed.), pp. 185–215. Springer-Verlag, Berlin, Heidelberg.

Machemer, H., and Ogura, A. (1979). Ionic conductances of membranes in ciliated and deciliated *Paramecium*. *J. Physiol.* **296,** 49–60.

Majima, T., Hamasaki, T., and Arai, T. (1986). Increase in cellular cyclic GMP level by potassium stimulation in *Paramecium tetraurelia*. *Experientia* **42,** 62–64.

Marengo, F. D., and Monck, J. R. (2000). Development and dissipation of Ca^{2+} gradients in adrenal chromaffin cells. *Biophys. J.* **79,** 1800–1820.

Martin, T. F. J. (2003). Tuning exocytosis for speed: Fast and slow modes. *Biochim. Biophys. Acta* **1641,** 157–165.

Matsumoto, M., Solzin, J., Helbig, A., Hagen, V., Ueno, S.-I., Kawase, O., Maruyama, Y., Ogiso, M., Godde, M., Minakata, H., Kaupp, U. B., Hoshi, M., and Weyand, I. (2003). A sperm-activating peptide controls a cGMP-signaling pathway in starfish sperm. *Dev. Biol.* **260,** 314–324.

Mayer, A. (2002). Membrane fusion in eukaryotic cells. *Annu. Rev. Cell Dev. Biol.* **18,** 289–314.

Miyawaki, A., Sawano, A., and Kogure, T. (2003). Lighting up cells: Labelling proteins with fluorophores. *Nature Cell Biol. Suppl.* **2003,** S1–S7.

Moffat, K., and Henderson, R. (1995). Freeze trapping of reaction intermediates. *Curr. Op. Struct. Biol.* **5,** 656–663.

Mohamed, I., Husser, M., Sehring, I., Hentschel, J., Hentschel, C., and Plattner, H. (2003). Refilling of cortical calcium stores in *Paramecium* cells: *In situ* analysis in correlation with store-operated calcium influx. *Cell Calcium* **34,** 87–96.

Mohamed, I., Klauke, N., Hentschel, J., Cohen, J., and Plattner, H. (2002). Functional and fluorochrome analysis of an exocytotic mutant yields evidence of store-operated Ca^{2-} influx in *Paramecium*. *J. Membr. Biol.* **187,** 1–14.

Montell, C. (2005). The latest waves in calcium signaling. *Cell* **122,** 157–163.

Moor, H. (1987). Theory and practice of high pressure freezing. *In* "Cryotechniques in Biological Electron Microscopy" (R. A. Steinbrecht and K. Zierold, Eds.), pp. 175–191. Springer-Verlag, Berlin, Heidelberg, New York.

Muallem, S. (2005). Decoding Ca^{2-} signals: A question of timing. *J. Cell Biol.* **170,** 173–175.

Müller, S., Diederichs, K., Breed, J., Kissmehl, R., Hauser, K., Plattner, H., and Welte, W. (2002). Crystal structure analysis of the exocytosis-sensitive phosphoprotein, pp63/parafusin (phosphoglucomutase), from *Paramecium* reveals significant conformational variability. *J. Mol. Biol.* **315,** 141–153.

Naitoh, Y., and Kaneko, H. (1972). Reactivated triton-extracted models of *Paramecium*: Modification of ciliary movements by calcium ions. *Science* **176,** 523–524.

Nakaoka, Y., and Machemer, H. (1990). Effects of cyclic nucleotides and intracellular Ca on voltage-activated ciliary beating in *Paramecium*. *J. Comp. Physiol. A* **166,** 401–406.

Narayanan, B., Islam, M. N., Bartelt, D., and Ochs, R. S. (2003). A direct mass-action mechanism explains capacitative calcium entry in Jurkat and skeletal L6 muscle cells. *J. Biol. Chem.* **278,** 44188–44196.

Neher, E. (1995). The use of Fura-2 for estimating Ca buffers and Ca fluxes. *Neuropharmacology* **34,** 1423–1442.

Neher, E. (1998). Vesicle pools and Ca^{2+} microdomains: New tools for understanding their roles in neurotransmitter release. *Neuron* **20,** 389–399.

Neher, E., and Marty, A. (1982). Discrete changes of cell membrane capacitance observed under conditions of enhanced secretion in bovine adrenal chromaffin cells. *Proc. Natl. Acad. Sci. USA* **79,** 6712–6716.

Noguchi, M., Sasaki, J.-Y., Kamachi, H., and Inoue, H. (2003). Protein phosphatase 2C is involved in the cAMP-dependent ciliary control in *Paramecium caudatum*. *Cell Motil. Cytoskel.* **54,** 95–104.

Palfrey, H. C., and Artalejo, C. R. (1998). Vesicle recycling revisited: Rapid endocytosis may be the first step. *Neuroscience* **83,** 969–989.

Parekh, A. B., and Penner, R. (1997). Store depletion and calcium influx. *Physiol. Rev.* **77,** 901–930.

Parekh, A. B., and Putney, J. W. (2005). Store-operated calcium channels. *Physiol. Rev.* **85,** 757–810.

Park, M. K., Petersen, O. H., and Tepikin, A. V. (2000). The endoplasmic reticulum as one continuous Ca^{2+} pool: Visualization of rapid Ca^{2+} movements and equilibration. *EMBO J.* **19,** 5729–5739.

Pech, L. L. (1995). Regulation of ciliary motility in *Paramecium* by cAMP and cGMP. *Comp. Biochem. Physiol.* **111A,** 31–37.

Pernberg, J., and Machemer, H. (1995). Fluorimetric measurement of the intracellular free Ca^{2+}-concentration in the ciliate *Didinium nasutum* using Fura-2. *Cell Calcium* **18,** 484–494.

Peters, C., Bayer, M. J., Bühler, S., Andersen, J. S., Mann, M., and Mayer, A. (2001). Trans-complex formation by proteolipid channels in the terminal phase of membrane fusion. *Nature* **409,** 581–583.

Petersen, O. H., Michalak, M., and Verkhratsky, A. (2005). Calcium signalling: Past, present and future. *Cell Calcium* **38,** 161–169.

Pezzati, R., Meldolesi, J., and Grohovaz, F. (2001). Ultra rapid calcium events in electrically stimulated frog nerve terminals. *Biochem. Biophys. Res. Commun.* **285,** 724–727.

Plattner, H. (1981). Membrane behaviour during exocytosis. *Cell Biol. Int. Rep.* **5,** 435–459.

Plattner, H., and Bachmann, L. (1982). Cryofixation: A tool in biological ultrastructural research. *Int. Rev. Cytol.* **79,** 237–304.

Plattner, H., and Hardt, M. (2000). Time resolved EM, ESI and EDX analylsis of exo-endocytosis within the sub-second time range in a synchronous system. *In* "Proceedings 12th European Congress on Electron Microsccopy" (L. Frank and F. Ciampor, Eds.), pp. B377–B380. Czech. Soc. Electron Microsc., Brno (CZ).

Plattner, H., and Kissmehl, R. (2003a). Dense-core secretory vesicle docking and exocytotic membrane fusion in *Paramecium* cells. *Biochim. Biophys. Acta (Mol. Cell Res.)* **1641,** 183–193.

Plattner, H., and Kissmehl, R. (2003b). Molecular aspects of membrane trafficking in *Paramecium*. *Int. Rev. Cytol.* **232,** 185–216.

Plattner, H., and Kissmehl, R. (2005). Molecular aspects of rapid, reversible, Ca^{2+}-dependent de-phosphorylation of pp63/parafusin during stimulated exo-endocytosis in *Paramecium* cells. *Cell Calcium* **38,** 319–327.

Plattner, H., and Klauke, N. (2001). Calcium in ciliated protozoa: Sources, regulation, and calcium-regulated cell functions. *Int. Rev. Cytol.* **201,** 115–208.

Plattner, H., and Zingsheim, H. P. (1983). Electron microscopic methods in cellular and moleeular biology. *Sub-Cell. Biochem.* **9,** 1–236.

Plattner, H., Fischer, W. M., Schmitt, W. W., and Bachmann, L. (1972). Freeze-etching of cells without cryoprotectants. *J. Cell Biol.* **53,** 116–126.

Plattner, H., Knoll, G., and Erxleben, C. (1992). The mechanics of biological membrane fusion. Merger of aspects from electron microscopy and patch-elamp analysis. *J. Cell Sci.* **103,** 613–618.

Plattner, H., Knoll, G., and Pape, R. (1993). Synchronization of different steps of the secretory cycle in *Paramecium tetraurelia*: Trichocyst exocytosis, exocytosis-coupled endocytosis and intracellular transport. *In* "Membrane Traffic in Protozoa" (H. Plattner, Ed.), pp. 123–148. JAI Press, Greenwich (CT), London.

Plattner, H., Braun, C., and Hentschel, J. (1997). Facilitation of membrane fusion during exocytosis and exocytosis-coupled endocytosis and acceleration of "ghost" detachment in *Paramecium* by extracellular calcium. *J. Membr. Biol.* **158,** 197–208.

Plattner, H., Diehl, S., Husser, M. R., and Hentschel, J. (2006). Sub-second calcium coupling between outside medium and subplasmalemmal stores during overstimulation/depolarisation-induced ciliary beat reversal in *Paramecium* cells. *Cell Calcium* **39,** 509–516.

Plattner, H., Matt, H., Kersken, H., Haacke, B., and Stürzl, R. (1984). Synchronous exocytosis in *Paramecium* cells. I. A novel approach. *Exp. Cell Res.* **151,** 6–13.

Plattner, H., Stürzl, R., and Matt, H. (1985). Synchronous exocytosis in *Paramecium* cells. IV. Polyamino-compounds as potent trigger agents for repeatable trigger-redocking cycles. *Eur. J. Cell Biol.* **36,** 32–37.

Politz, J. C. (1999). Use of caged fluorochromes to track macromolecular movement in living cells. *Trends Cell Biol.* **9,** 284–287.

Pollard, T. D., Maupin, P., Sinard, J., and Huxley, H. E. (1990). A stopped-flow/rapid-freezing machine with millisecond time resolution to prepare intermediates in biochemical reactions for electron microscopy. *J. Electron Microsc. Techn.* **16,** 160–166.

Pollard, T. D., Bhandari, D., Maupin, P., Wachsstock, D., Weeds, A. G., and Zot, H. G. (1993). Direct visualization by electron microsocpy of the weakly bound intermediates in the actomyosin adenosine triphosphatase cycle. *Biophys. J.* **64,** 454–471.

Pozzo-Miller, L. D., Pivovarova, N. B., Connor, J. A., Reese, T. S., and Andrews, S. B. (1999). Correlated measurements of free and total intracellular calcium concentration in central nervous system neurons. *Microsc. Res. Techn.* **46,** 370–379.

Pozzo-Miller, L. D., Connor, J. A., and Andrews, S. B. (2000). Microheterogeneity of calcium signalling in dendrites. *J. Physiol.* **525,** 53–61.

Preston, R. R., and Saimi, Y. (1990). Calcium ions and the regulation of motility in *Paramecium*. *In* "Ciliary and Flagellar Membranes" (R. A. Bloodgood, Ed.), pp. 173–200. Plenum Press, New York, London.

Purich, D. L. (Ed.). (2002). Enzyme Kinetics and Mechanism. *Methods Enzymol.* **354,** 354.

Putney, J. W., Broad, L. M., Brun, F. J., Lievremont, J. P., and Bird, G. S. J. (2001). Mechanisms of capacitative calcium entry. *J. Cell Sci.* **114,** 2223–2229.

Randriamampita, C., and Trautmann, A. (2004). Ca^{2+} signals and T lymphocytes. "New mechanisms and functions in Ca^{2+} signalling". *Biol. Cell* **96,** 69–78.

Reimer, L. (1998). "Scanning Electron Microscopy. Physics of Image Formation and Microanalysis," 2nd ed. Springer Verlag, Berlin, Heidelberg, New York.

Richards, D. A., Bai, J., and Chapman, E. R. (2005). Two modes of exocytosis at hippocampal synapses revealed by rate of FM1-43 efflux from individual vesicles. *J. Cell Biol.* **168,** 929–939.

Rizzuto, R., and Pozzan, T. (2006). Microdomains of intracellular Ca^{2+}: Molecular determinants and functional consequences. *Physiol. Rev.* **86,** 369–408.

Robert, V., Gurlini, P., Tosello, V., Nagai, T., Miyawaki, A., DiLisa, F., and Pozzan, T. (2001). Beat-to-beat oscillations of mitochondrial $[Ca^{2+}]$ in cardiac cells. *EMBO J.* **20,** 4998–5007.

Rosado, J. A., and Sage, S. O. (2000). The actin cytoskeleton in store-mediated calcium entry. *J. Physiol.* **526,** 221–229.

Rosado, J. A., Redondo, P. C., Salido, G. M., Sage, S. O., and Pariente, J. A. (2005). Cleavage of SNAP-25 and VAMP-2 impairs store-operated Ca^{2+} entry in mouse pancreatic acinar cells. *Am. J. Physiol. (Cell Physiol.)* **288,** C214–C221.

Rosenboom, H., and Lindau, M. (1994). Exo-endocytosis and closing of the fission pore during endocytosis in single pituitary nerve terminals internally perfused with high calcium concentrations. *Proc. Nat. Acad. Sci. USA* **91,** 5267–5271.

Rothman, J. E., and Söllner, T. H. (1997). Throttles and dampers: Controlling the engine of membrane fusion. *Science* **276,** 1212–1213.

Rudolf, R., Mongillo, M., Rizzuto, R., and Pozzan, T. (2004). Looking forward to seeing calcium. *Nature Rev. Microsc. Coll.* **2004,** 36–43.

Saiki, Y., and Ikemoto, N. (1999). Coordination between Ca^{2+} release and subsequent re-uptake in the sarcoplasmic reticulum. *Biochemistry* **38,** 3112–3119.

Sakato, M., and King, S. M. (2003). Calcium regulates ATP-sensitive microtubule binding by *Chlamydomonas* outer arm dynein. *J. Biol. Chem.* **278,** 43571–43579.

Salaün, C., James, D. J., Greaves, J., and Chamberlain, L. H. (2004). Plasma membrane targeting of exocytic SNARE proteins. *Biochim. Biophys. Acta* **1693,** 81–89.

Schilde, C., Wassmer, T., Mansfeld, J., Plattner, H., and Kissmehl, R. (2006). A multigene family encoding R-SNAREs in the ciliate *Paramecium tetraurelia*. *Traffic* **7,** 440–455.

Schmitz, M., and Zierold, K. (1989). X-ray microanalysis of ion changes in fast processes of cells, as exemplified by trichocyst exocytosis of *Paramecium caudatum*. *In* "Electron Microscopy of Subcellular Dynamics" (H. Plattner, Ed.), pp. 325–339. CRC Press, Boca Raton (FL).

Schneggenburger, R., and Neher, E. (2005). Presynaptic calcium and control of vesicle fusion. *Curr. Op. Neurobiol.* **15,** 266–274.

Schultz, J. E., and Klumpp, S. (1993). Cyclic nucleotides and calcium signaling in *Paramecium*. *Adv. Sec. Mess. Phosphoprot. Res.* **27,** 25–46.

Séron, K., Tieaho, V., Prescianotto-Baschong, C., Aust, T., Blondel, M.-O., Guillaud, P., Devilliers, G., Rossanese, O. W., Glick, B. S., Riezman, H., Keränen, S., and Haguenauer-Tsapis, R. (1998). A yeast t-SNARE involved in endocytosis. *Mol. Biol. Cell* **9,** 2873–2889.

Shattock, M. J., Miller, J. I. A., Marchant, C. L., Foreman, M. A., Ford, D. J., Bray, D. G., Waldron, C. B., Chambers, D. J., and Warley, A. (1998). A cryoclamp for the rapid

cryofixation of the isolated blood-perfused rabbit cardiac papillary muscle preparation at predefined times during the contraction cycle. *J. Microscopy* **192,** 269–279.

Sitte, H. (1996). Advanced instrumentation and methodology related to cryoultramicrotomy: A review. *Scanning Microsc. Suppl.* **10,** 387–466.

Sklar, L. A., Edwards, B. S., Graves, S. W., Nolan, J. P., and Prossnitz, E. R. (2002). Flow cytometric analysis of ligand-receptor interactions and molecular assemblies. *Annu. Rev. Biophys. Biomol. Struct.* **31,** 97–119.

Söllner, T. H. (2003). Regulated exocytosis and SNARE function. *Mol. Membr. Biol.* **20,** 209–220.

Somlyo, A. V., Gonzales-Serratos, H., Shuman, H., McClellan, G., and Somlyo, A. P. (1981). Calcium release and ion changes in the sarcoplasmic reticulum of tetanized muscle: An electron-probe study. *J. Cell Biol.* **90,** 577–594.

Stelly, N., Mauger, J. P., Kéryer, G., Claret, M., and Adoutte, A. (1991). Cortical alveoli of *Paramecium*: A vast submembraneous calcium storage compartment. *J. Cell Biol.* **113,** 103–112.

Stephens, D. J., and Allan, V. J. (2003). Light microscopy techniques for live cell imaging. *Science* **300,** 82–86.

Stuermer, C. A. O., Langhorst, M. F., Wiechers, M. F., Legler, D. F., Hannbeck von Hanwehr, S., Guse, A. H., and Plattner, H. (2004). PrP^c capping in T cells promotes its association with the lipid raft proteins reggie-1 and reggie-2 and leads to signal transduction. *FASEB J.* **18,** 1731–1733, online 10.1096/fj.04-2150fje.

Sun, J. Y., and Wu, L. G. (2001). Fast kinetics of exocytosis revealed by simultaneous measurements of presynaptic capacitance and postsynaptic currents at a central synapse. *Neuron* **30,** 171–182.

Takahashi, A., Camacho, P., Lechleiter, J. D., and Herman, B. (1999). Measurement of intracellular calcium. *Physiol. Rev.* **79,** 1089–1125.

Tamm, S. (1994). Ca^{2+} channels and signalling in cilia and flagella. *Trends Cell Biol.* **4,** 305–310.

Tamm, S. L., and Terasaki, M. (1994). Visualization of calcium transients controlling orientation of ciliary beat. *J. Cell Biol.* **125,** 1127–1135.

Taraska, J. W., Perrais, D., Ohara-Imaizumi, M., Nagamatsu, S., and Almers, W. (2003). Secretory granules are recaptured largely intact after stimulated exocytosis in cultured endocrine cells. *Proc. Natl. Acad. Sci. USA* **100,** 2070–2075.

Tareilus, E., Schoch, J., Adams, M., and Breer, H. (1993). Analysis of rapid calcium signals in synaptosomes. *Neurochem. Int.* **23,** 331–341.

Taylor, K. A., Schmitz, H., Reedy, M. C., Goldman, Y. E., Franzini-Armstrong, C., Sasaki, H., Tregear, R. T., Poole, K., Lucaveche, C., Edwards, R. J., Chen, L. F., Winkler, H., and Reedy, M. K. (1999). Tomographic 3D reconstruction of quick-frozen, Ca^{2+}-activated contracting insect flight muscle. *Cell* **99,** 421–431.

Teng, H., and Wilkinson, R. S. (2003). 'Delayed' endocytosis is regulated by extracellular Ca^{2+} in snake motor boutons. *J. Physiol.* **551,** 103–114.

Thomas, P., Surprenant, A., and Almers, W. (1990). Cytosolic Ca^{2+}, exocytosis, and endocytosis in single melanotrophs of the rat pituitary. *Neuron* **5,** 723–733.

Thomas, P., Wong, J. G., Lee, A. K., and Almers, W. (1993). A low affinity Ca^{2+} receptor controls the final steps in peptide secretion from pituitary melanotrophs. *Neuron* **11,** 93–104.

Toomre, D., and Manstein, D. J. (2001). Lighting up the cell surface with evanescent wave microscopy. *Trends Cell Biol.* **11,** 298–303.

Torri-Tarelli, F., Grohovaz, F., Fesce, R., and Ceccarelli, B. (1985). Temporal coincidence between synaptic vesicle fusion and quantal secretion of acetylcholine. *J. Cell Biol.* **101,** 1386–1399.

Tsien, R. Y. (2005). Building and breeding molecules to spy on cells and tumors. *FEBS Lett.* **579,** 927–932.

Unwin, N. (1995). Acetylcholine receptor channel imaged in the open state. *Nature* **373,** 37–43.

Vanhecke, D., Graber, W., Herrmann, G., Al-Amoudi, A., Eggli, P., and Studer, D. (2003). A rapid microbiopsy system to improve the preservation of biological samples prior to high-pressure freezing. *J. Microscopy* **212,** 3–12.

Walker, M., Zhang, X.-Z., Jiang, W., Trinick, J., and White, H. D. (1999). Observation of transient disorder during myosin subfragment-1 binding to actin by stopped-flow fluorescence and millisecond time resolution electron cryomicroscopy: Evidence that the start of the crossbridge power stroke in muscle has variable geometry. *Proc. Natl. Acad. Sci. USA* **96,** 465–470.

Wang, C.-T., Bai, J., Chang, P. Y., Chapman, E. R., and Jackson, M. B. (2006). Synaptotagmin-Ca^{2+} triggers two sequential steps in regulated exocytosis in rat PC12 cells: Fusion pore opening and fusion pore dilation. *J. Physiol.* **570,** 295–307.

Wassmer, T., Froissard, M., Plattner, H., Kissmehl, R., and Cohen, J. (2005). The vacuolar proton-ATPase plays a major role in several membrane-bounded organelles in *Paramecium*. *J. Cell Sci.* **118,** 2813–2825.

Wendt-Gallitelli, M. F., and Isenberg, G. (1991). Total and free myoplasmic calcium during a contraction cycle: X-ray microanalysis in guinea-pig ventricular myocytes. *J. Physiol.* **435,** 349–372.

White, H. D., Walker, M. L., and Trinick, J. (1998). A computer-controlled spraying-freezing apparatus for millisecond time-resolution electron cryomicroscopy. *J. Struct. Biol.* **121,** 306–313.

Wood, C. D., Nishigaki, T., Furuta, T., Baba, S. A., and Darszon, A. (2005). Real-time analysis of the role of Ca^{2+} in flagellar movement and motility in single sea urchin sperm. *J. Cell Biol.* **169,** 725–731.

Wu, L. G. (2004). Kinetic regulation of vesicle endocytosis at synapses. *Trends Neurosci.* **27,** 548–554.

Yang, X., Pingyong, X., and Xu, T. (2005). A new pair for inter- and intra-molecular FRET measurement. *Biochem. Biophys. Res. Commun.* **330,** 914–920.

Yang, W. Q., Braun, C., Plattner, H., Purvee, J., and Van Houten, J. L. (1997). Cyclic nucleotides in glutamate chemosensory signal transduction of *Paramecium*. *J. Cell Sci.* **110,** 2567–2572.

Yarar, D., Waterman-Storer, C. M., and Schmid, S. L. (2005). A dynamic actin cytoskeleton functions at multiple stages of clathrin-mediated endocytosis. *Mol. Biol. Cell* **16,** 964–975.

Yuste, R. (2005). Fluorescence microscopy today. *Nature Meth.* **2,** 902–909.

Zoghbi, M. E., Copello, J. A., Villalba-Galea, C. A., Vélez, P., Diaz Sylvester, P. L., Bolanos, P., Marcano, A., Fill, M., and Escobar, A. L. (2004). Differential Ca^{2+} and Sr^{2+} regulation of intracellular divalent cations release in ventricular myocytes. *Cell Calcium* **36,** 119–134.

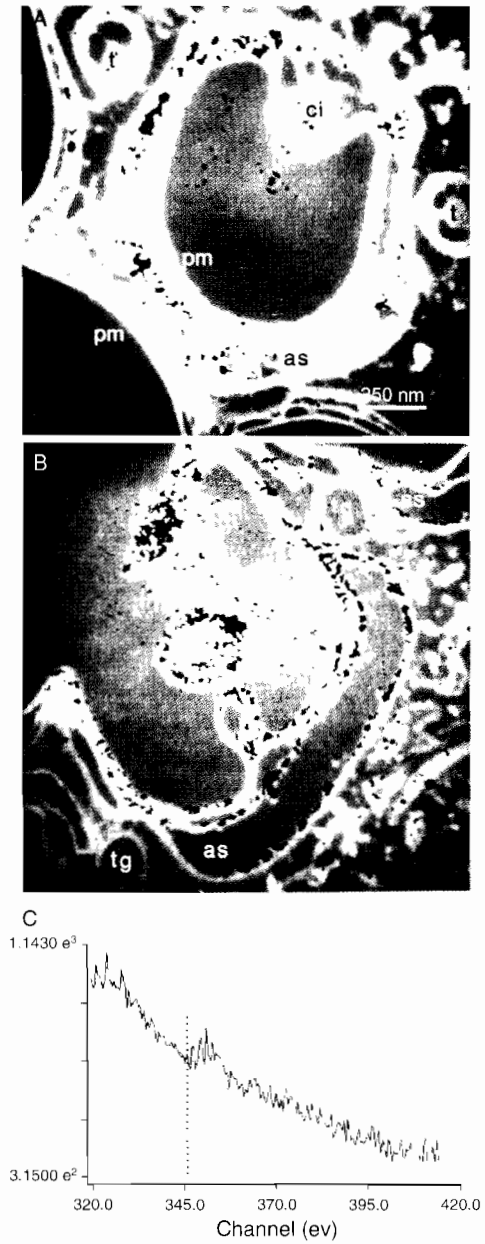

PLATTNER AND HENTSCHEL FIG. 7 ESI-based Ca-analysis in *Paramecium*. (A) before and (B) 80 ms after exocytosis stimulation. (C) is the energy loss spectrum with the Ca signal. For Ca imaging (displayed in red false color), as shown in (A) and (B), net signals after background subtraction have been used. Alveolar sacs (as) show Ca signals throughout their extension in (A), whereas after stimulation (B) Ca signals in alveolar sacs are restricted to their borders, with additional signals along the plasmamembrane (pm) and in cilia (ci). No Ca signals are seen in trichocysts (t) or trichocyst ghosts (tg). From Knoll *et al.* (1993). *Cell Calcium*, **14**, 173–183 by copyright permission of Elsevier.

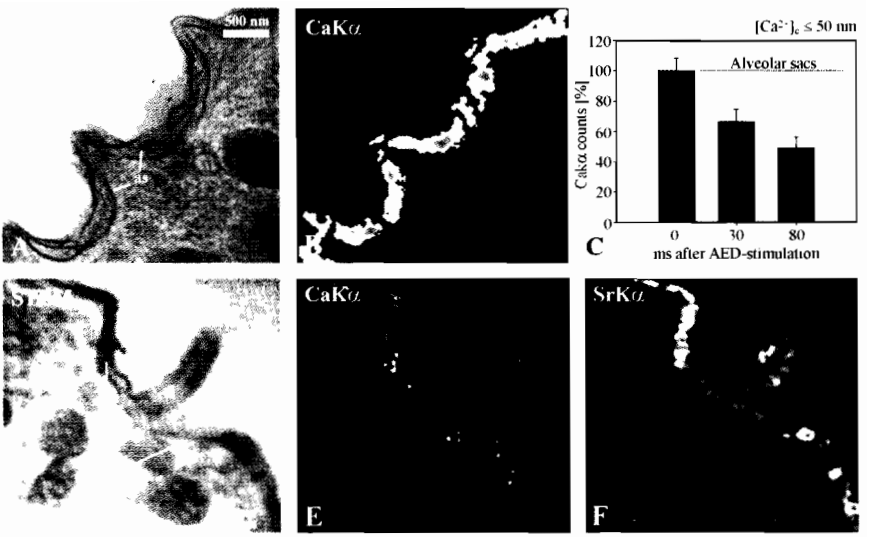

PLATTNER AND HENTSCHEL FIG. 9 EDX-based imaging of Ca and of Sr during exocytosis stimulation in *Paramecium*. (A) STEM image of unstimulated cell, with corresponding CaKα-distribution image (B), showing restriction of signals (in false colors, with some red hot spots) to alveolar sacs (as) and absence, for example from cilia (ci). (C) Decrease of net CaKα signals in alveolar sacs during exocytosis stimulation executed at $[Ca^{2+}]_c$ slightly below intracellular resting levels (see text). (D, E, F): STEM (D), CaKα (E) and SrKα image (F) of a cell AED-stimulated at low $[Ca^{2-}]_c$ in presence of an excess of Sr^{2+} added during stimulation. Note disappearance of the CaKα signal (E), whereas the SrKα signal emerges in alveolar sacs (and in the cilium). This clearly documents rapid release of Ca^{2+} from cortical stores and substitution of Sr^{2+} for Ca^{2+} in these stores, respectively, during exocytosis stimulation. (A–C) is from Hardt and Plattner. (2000). *Euro. J. Cell Biol.* **79**, 642–652 by copyright permission of Elsevier; (D–F) from Hardt and Plattner. (1999). *J. Struct. Biol.* **128**, 187–199 by copyright permission of Elsevier.